# Energy recovery from sugarcane bagasse under varying microwave-assisted pyrolysis conditions

**Scarlett Allende[1], Graham Brodie[1], Mohan V. Jacob[1*]**

[1]Electronics Material Lab, College of Science and Engineering, James Cook University, Townsville QLD 4811 Australia

Corresponding author: email: Mohan.Jacob@jcu.edu.au

## Abstract

Waste management and utilisation of waste is a major global issue. This study investigated the influential parameters on the energy recovery from the sugarcane bagasse breakdown under microwave pyrolysis conditions. The byproduct yield is optimised from 45 different combinations of microwave power, reaction time and microwave susceptor. The surface methodology, energy efficiency and byproduct quality were studied. Low power, less microwave susceptor and longer residence time are the desirable conditions for high biochar yield due to the gradual thermal decomposition of the biomass and low heating rates. The highest bio-oil yield was obtained from higher microwave power and lower residence time. The excess pyrolysis temperature generated by the higher microwave power and higher microwave susceptor addition produces higher temperatures beyond the optimal condition for bio-oil production. This phenomenon is relative to the self-gasification of the biochar during the high pyrolysis power, contributing to the formation of $H_2$, CO and $CH_4$.

**Keywords:** Microwave pyrolysis; sugarcane bagasse, biochar, bio-oil, biogas

**Graphical abstract**

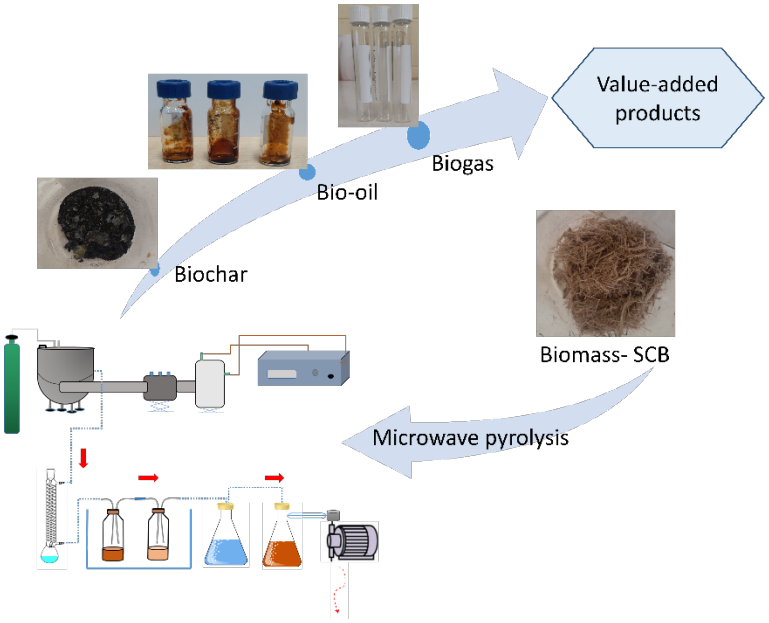


## 1. Introduction

Excessive use of non-renewable energy sources, depletion of fossil fuels and population growth cause a significant impact on climate change, air contamination and the economy (Daneshmandi et al., 2022; Ferrari et al., 2022). Fossil fuel combustion generates around 98% of human carbon dioxide emissions (Prasad & Ingle, 2019). On the other hand, the disposal of different types of waste produces significant greenhouse emissions, like methane and carbon dioxide gas, contributing to the rise in atmospheric temperature and global climate change (Liu et al., 2021). Some biomass sources comprise agricultural waste, wood, animal and crop residues, food waste, municipal waste, algae, plastics and cooking oil (Cai et al., 2021; Lee et al., 2019; Wang et al., 2021). Globally, 23.7 million tons of agroindustrial biomass is generated per day (Duque-Acevedo et al., 2020). Hence, the deficit of energy resources, high fossil fuel demand, and greenhouse gas (GHG) emissions make bioenergy a promising alternative for clean energy production (Daneshmandi et al., 2022; Mierzwa-Hersztek et al., 2019).

Bioenergy is acknowledged as a renewable and sustainable energy source due to the energy conversion of lignocellulosic biomass having a lower-carbon life cycle than fossil fuel, generating heat, electricity and fuels with low environmental hazards (Daneshmandi et al., 2022; Le Pera et al., 2022). Biomass can be converted to energy by two methods: thermochemical and biochemical processes. The thermochemical method comprises

combustion, gasification, and conventional and microwave pyrolysis (Liu et al., 2022). Anaerobic digestion and microbial fermentation are biochemical conversion methods (Le Pera et al., 2022; Li et al., 2022b). The selection of biomass conversion method is crucial for synthesizing by-products and recovering energy (Lee et al., 2019; Li et al., 2022b). The nature of biomass is a relevant factor in choosing the appropriate energy conversion technology because of its structural and chemical composition. For example, the decomposition of lignocellulosic biomass occurs faster in a thermochemical method than in a biological conversion due to the high heating efficiency (Arpia et al., 2021; Huang et al., 2016). The fibre composition of lignocellulosic biomass is cellulose, hemicellulose, and lignin. The range of fibre compounds in these materials depends on the nature of the biomass. For example, sugarcane bagasse has higher cellulose content (46.55 wt%) than rice husk (30.42 wt%) (Huang et al., 2016; Lo et al., 2017).

Conventional and microwave pyrolysis implies the thermochemical breakdown of the biomass in the absence of an oxidizing agent for producing biochar, bio-oil and biogas (Arpia et al., 2021). The main difference between microwave and conventional pyrolysis is the heating method; the microwave method involves volumetric heating, and conventional pyrolysis is conduction/convection heating (Selvam S & Paramasivan, 2022; Shukla et al., 2019). Conventional pyrolysis is achieved using a bath furnace with high thermal inertia and low electricity conversion efficiency (Arpia et al., 2021). Microwave-assisted pyrolysis has higher efficiency in the heating process because energy transfer is through the interaction of the molecules inside the biomass rather than by heat transfer from external sources (Li et al., 2022a; Zi et al., 2019). The advantages of microwave heating are shorter reaction time, better distribution and control over the heating, non-contact heating, and quick start-up and stopping mechanism (Arpia et al., 2021; Yu et al., 2022). However, microwave pyrolysis requires a microwave susceptor to absorb the electromagnetic radiation and start the energy transfer (Suriapparao et al., 2018).

Some types of biomass present poor dielectric heating properties, which involve lower absorption of microwave energy. In the case of dielectric loss tangent (tanδ) of polyethylene, polypropylene, fir plywood, wood polymer, sludge, and PVC are 0.0001, 0.0003, 0.01, 0.03 and 0.035, 0.0056, respectively (Zhang et al., 2017a; Zhang et al., 2017b). Therefore, the addition of a microwave susceptor (M.S) is necessary to transform the electromagnetic energy into heat to be transferred to the biomass, allowing the pyrolysis reaction to initiate (Suriapparao et al., 2018; Zi et al., 2019). The ratio of microwave susceptors, biomass

feedstock volume and intrinsic biomass properties influence the heating rate of the conversion process and the biochar, bio-oil, and biogas yield. The high addition of microwave susceptor at an elevated reaction temperature can produce a secondary thermal breakdown of non-condensable volatiles into permanent gaseous compounds, increasing biogas yield but reducing bio-oil production (Shi et al., 2020; Zhang et al., 2017a; Zhang et al., 2017b). Ranges of tanδ in diverse microwave susceptors are between 0.02 and 1.05 (Ellison et al., 2017; Zhang et al., 2017a; Zhang et al., 2017b). Representative absorber materials are SiC, activated carbon, biochar, graphite, glycerol, fly ash and water (Zhang et al., 2022; Zhang et al., 2017a; Zhang et al., 2017b). The selection of a suitable microwave susceptor contributes to a significant difference in the heating rate, microwave assimilation capacity of bulk biomass, energy consumption (microwave energy system) and by-product quality (Selvam S & Paramasivan, 2022; Zhang et al., 2017a).

Several studies have reported the by-products optimisation of diverse biomass using microwave pyrolysis, e.g., horse manure (Mong et al., 2021), oil palm (Idris et al., 2022), plastic (Suriapparao et al., 2022), corn cob (Quillope et al., 2021), flax shives (Ubiera et al., 2021), sugarcane bagasse (S & Paramasivan, 2021), bamboo, gumwood and pine (Shi et al., 2020). However, most studies did not consider: (i) processing a higher biomass volume (over 50 grams); (ii) evaluating the impact of the optimised by-product on global energy recovery; (iii) assessing operating parameters on the quality of the target by-product; (iv) integrating sustainable aspects (economic and environmental analysis) on global energy efficiency. These factors are relevant to investigate to fully understand the challenges that face energy recovery using a pilot-scale microwave system from the processing of sugarcane bagasse.

This study intended to investigate the influential parameters on the energy recovery of the breakdown of sugarcane bagasse under microwave pyrolytic conditions. The objectives of this research include: (i) identifying the optimal yield of by-products established by the experimental combination scenarios; (ii) evaluating the influential parameters on the characterisation and quality of by-products; (iii) assessing the impact of the target by-product on the total energy output and global energy recovery; (iv) techno-economic estimation of microwave pyrolysis system based on diverse operational conditions; and (v) do the carbon footprint of the SCB processing.

## 2. Experiments and Methods

### 2.1 Raw biomass material

Sugarcane bagasse (Wilmar, Queensland) was used as feedstock in microwave pyrolysis. The water content of the biomass was determined by grounding the sample into smaller sizes (0.2-0.5 mm) until obtaining a representative feedstock. Then, the SCB was exposed to 110ºC in an oven until attaining constant weight (~ 2 hours). The resulting moisture content was 10 wt%. Raw bagasse (wet condition) was used to determine proximate analysis. Table 1 shows the physicochemical properties of the raw biomass. The volatile matter, ash content and fixed carbon were 76 wt%, 4 wt% and 10 wt%, respectively. The high heating value (HHV) and low heating value (LHV) were estimated by the elemental composition of the biomass. The ultimate analysis indicates that carbon (41.93 wt%) and oxygen (53.39 wt%) are the most abundant elements in the sugarcane bagasse. The calculated HHV was 17.324 MJ/kg and LHV 13.863 MJ/kg. These values are relevant for the energy balance obtained from microwave pyrolysis.

Table 1: Physicochemical properties of raw sugarcane bagasse

| **Biomass raw material properties, wt%** | **Sugarcane bagasse** |
|---|---|
| **Moisture content** | 9.9 |
| **Ash Content** | 4 |
| **Volatile matter** | 76 |
| **Fixed carbon** | 10 |
| | |
| **Elemental composition, wt%** | |
| **C** | 41.93 |
| **H** | 5.47 |
| **N** | 0.21 |
| **O** | 53.39 |
| **HHV, MJ/kg** | 17.324 |
| **LHV, MJ/kg** | 13.863 |

The microwave absorbance of sugarcane bagasse is represented by the loss tangent (tanδ), which is around 0.161 (Liyana et al., 2012). Biomass moisture content directly impacts the tanδ value due to the high microwave absorbance of water (tanδ=0.12) (Zhang et al., 2017b). High moisture content can lead to a high tanδ value and increased bio-oil yield with an elevated aqueous fraction. Nevertheless, the moisture existing in the biomass is evaporated during the

microwave conversion process, generating bio-oil with high aqueous fractions and low heating value (Ethaib et al., 2020; Giorcelli et al., 2021; Zhang et al., 2017a).

Thermal degradation of the fibre composition of sugarcane bagasse starts between 200 ºC to 400 ºC (Najeeb et al., 2021). Below 100 ºC temperature, there is a mass loss associated with the moisture content of raw biomass (Gomes, 2018; Najeeb et al., 2021). Figure 1 shows the thermogravimetric curve of sugarcane bagasse used in the experiments. Studies in literature show a steady and gradual degradation of biomass when the temperature and power are sufficient to initiate the decomposition of the lignin component, which is between 350 ºC and 900 ºC (Dai et al., 2020; Shi et al., 2020; Zi et al., 2019). However, the thermal breakdown of hemicellulose and cellulose is quicker than the lignin component, e.g., between 250 ºC to 350 ºC and 350 ºC to 500 ºC, respectively (Dai et al., 2020; Zi et al., 2019). Therefore, using microwave pyrolysis, an optimal operating temperature of sugarcane bagasse is reported at over 400 ºC.

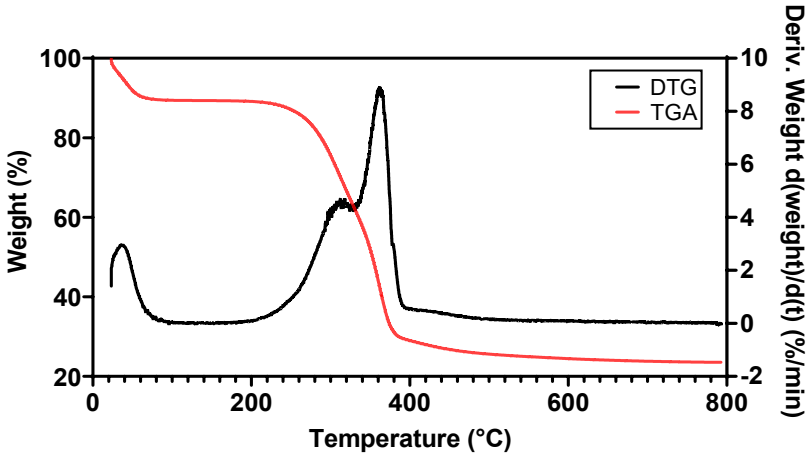


Figure 1: TGA and DTG of raw sugarcane bagasse

### 2.2 Microwave-assisted pyrolysis system and experimental procedure

Figure 2 illustrates the microwave-assisted pyrolysis mechanism. The custom-made prototype was designed to process up to 5 kilograms of biomass (pilot-scale production). The system consists of a 3 kW microwave generator, an auto-tuner for impedance matching, a chamber where the biomass is pyrolysed, a vacuum pump, and various condensers for collecting biogas and bio-oil. Once the system is loaded with the biomass, the air is removed from the pyrolysis system using the rotary vacuum pump and purged with nitrogen gas. Between 5 to 6 $Lmin^{-1}$ of nitrogen gas was applied, preserving an inert atmosphere during experiments. The negative pressure generated inside the chamber is around 25 to 10 kPa. The vacuum pump allows

extract gases from the reactor and then condenses them. Thus, more pyrolysis volatile condensation is generated under a vacuum environment, contributing to oil production. Ranges of microwave power and treatment time were established using the controller.

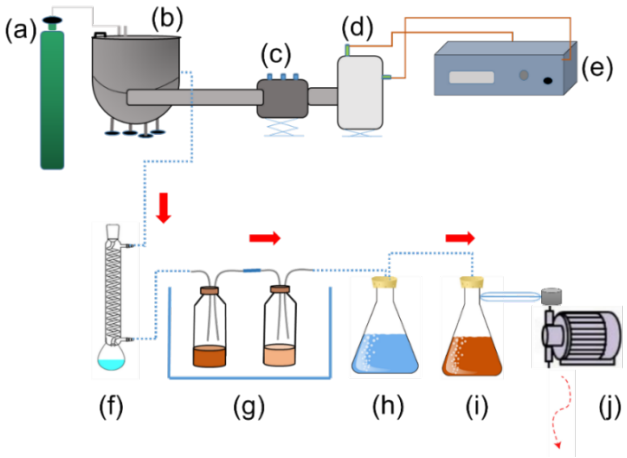


Figure 2: Components of microwave pyrolysis system. (a) nitrogen cylinder; (b) chamber; (c) tuner; (d) microwave generator; (e) controller; (f) condenser; (g) biogas flask in ice bath, (h) biogas purification flask; (i) bio-oil flask; (j) vacuum pump.

- **Characterisation technique and optimisation**

The elemental analysis was collected using CHNS FlashSMART, scanning electron microscopy performance on JEOL 7001F SEM. Thermogravimetric analysis (TGA) of SCB, biochar and bio-oil was conducted by Netzsch STA 449F3 Jupiter Simultaneous Thermal Analyser. Then, biochar surface area was measured using a micromeritics 3-flex surface and porosity analyser. Bio-oil functional groups were achieved by the ATD-GC-MS system (Toluene D8 as an internal standard). Biogas compounds analysis was developed using Shimadzu GC 2030 gas chromatograph. The optimisation analysis was conducted by response surface methodology (RSM), and its statistical model was designed using DOE and ANOVA (Minitab).

- **Synthesis of by-products**

This research was established by the modification of operating conditions, e.g., microwave power (kW), microwave-heating susceptor (%), and residence time (min). To identify the maximum by-product yield and their global energy efficiency, the same setting range in experimental conditions was considered for all 45 experiments, which produced the by-

products. The experimental design consisted of five microwave power ranges and three residence time and microwave susceptor additions. The SCB biochar generated from microwave pyrolysis was used as a microwave susceptor.

The input microwave power varied from 1 kW to 3 kW, increasing by 500 W in every experimental pyrolysis treatment. The residence times were 30, 40 and 50 minutes, and the microwave susceptor was 10%, 15% and 20%. A representative by-product yield was reached by repeating the experimental procedure four times. Therefore, the performance of each combination corresponds to the average of four pyrolysis runs. The selection of the optimal yield was based on the maximum value performed in the optimisation process of the three by-products attained in the lowest energy consumption (multivariate analysis of variance), with the independent variables of microwave power, susceptor volume and treatment time. Table 2 describes the experimental design for the synthesis of by-products.

Table 2: Experimental microwave setup

| Microwave power (kW) | Microwave susceptor, % | Reaction time, min |
|---|---|---|
| **1** | 10 | 30, 40 and 50 |
| | 15 | |
| | 20 | |
| **1.5** | 10 | 30, 40 and 50 |
| | 15 | |
| | 20 | |
| **2** | 10 | 30, 40 and 50 |
| | 15 | |
| | 20 | |
| **2.5** | 10 | 30, 40 and 50 |
| | 15 | |
| | 20 | |
| **3** | 10 | 30, 40 and 50 |
| | 15 | |
| | 20 | |

## 3. Result and discussion

### 3.1 Energy operational conditions

Figure 3 shows the resulting yield over the variation of operating conditions. Microwave energy consumption was calculated considering the input microwave power and the reaction time of the conversion process. The electrical energy was estimated by the relationship between energy consumption and the microwave unit efficiency (80%) (Shi et al., 2020). Then, the total input energy calculation involves biomass energy value (13.86 MJ/kg), biomass sample weight and electrical energy. The highest input energy value is 3.4 kWh, which consumed electricity at 3 kW for 50 minutes (2.5 kWh energy consumption).

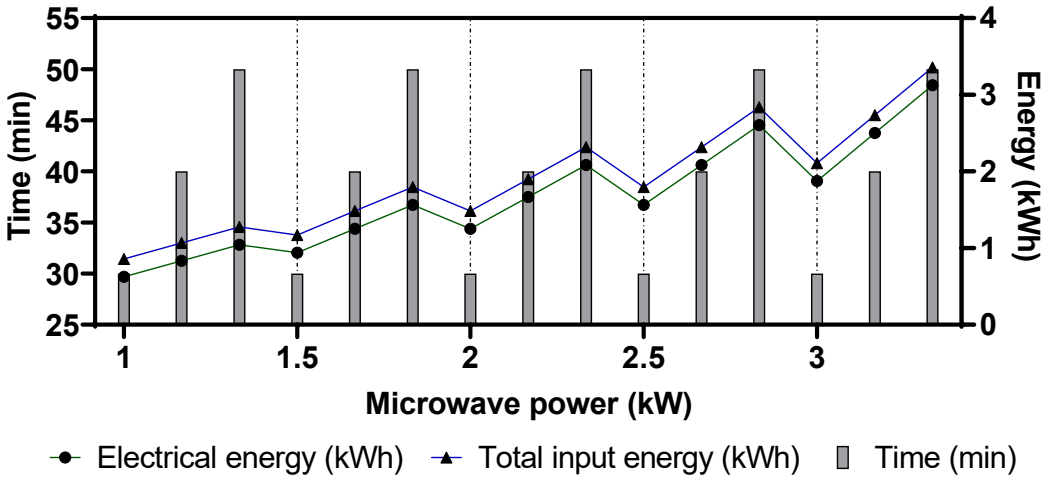


Figure 3: Operating conditions of microwave pyrolysis system.

### 3.2 By-products optimisation

#### 3.2.1 Biochar yield optimisation

Figure 4 shows biochar optimisation, and Table 3 describes the general linear model from the microwave pyrolysis process. The highest biochar yield was 38.1% at 1 kW for 40 minutes of treatment time and 10% microwave susceptor. The second highest yield was 37.9.1% at 1.5 kW for 30 minutes and 10% susceptor content. Literature report that low power, decreased microwave susceptor addition and longer residence time are the desirable conditions to obtain a higher biochar yield due to the gradual thermal decomposition of the biomass and low heating rates (Idris et al., 2022; Shi et al., 2020). This statement is confirmed by observing the biochar behaviour. When the reaction time was increased from 30 to 40 minutes at 1kW, biochar yield increased by 43%, considering a reduction of microwave susceptor from 20% to 10%. However, an excessive treatment time leads to the devolatilization of biomass and biochar by the excess pyrolysis temperature. Secondary pyrolysis reactions cause permanent gaseous formation, facilitating carbonization and reducing the biochar mass (Cong et al., 2018; Zhang et al., 2017a). For instance, when the residence time increased from 30 to 50 minutes, the biochar yield was reduced by 16%, assuming a 20% microwave susceptor and 1.5 kW.

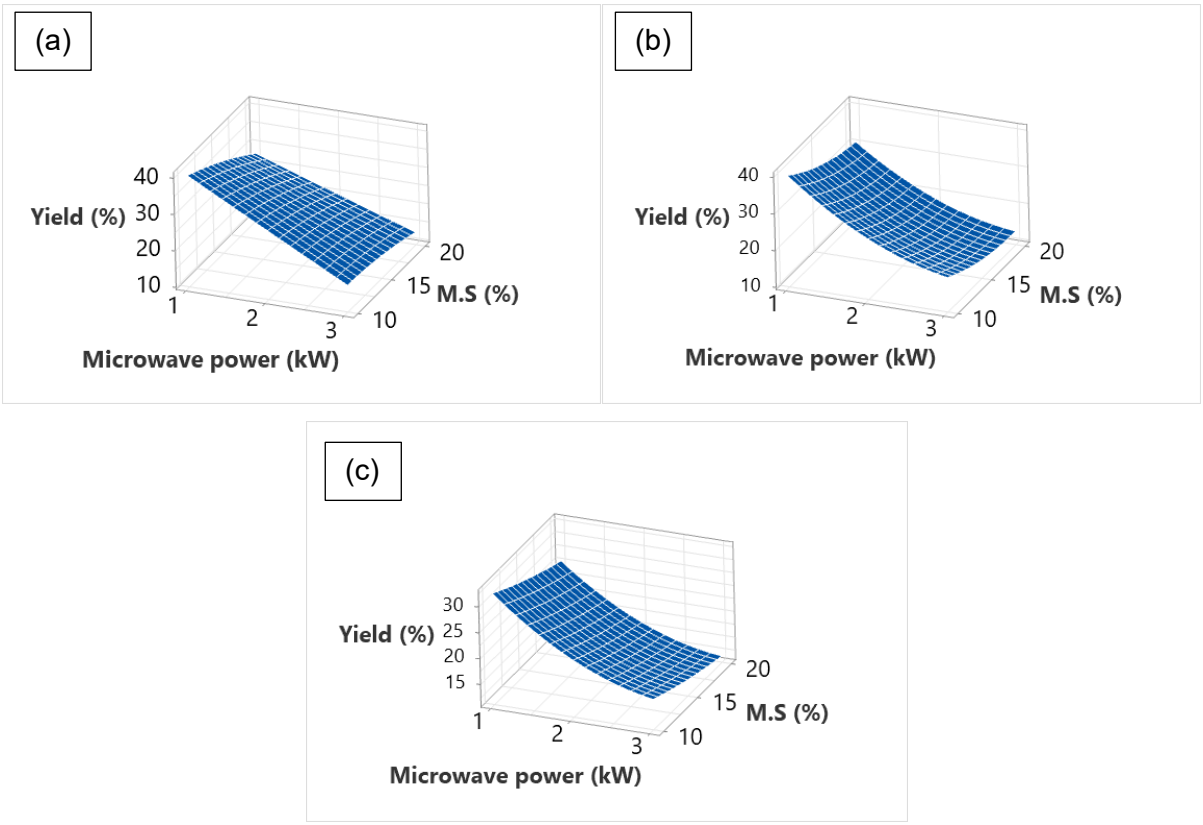


Figure 4: Response surface plot of biochar yield under (a) 30, (b) 40, and (c) 50 minutes of microwave pyrolysis.

Table 3: Regression equation of biochar yield versus reaction time, microwave power and microwave susceptor

| | R-sq (%) |
|---|---|
| B.C_Y(%)=22.685+1.906A+ 0.757B- 2.663C + 9.273D + 5.133 E- 1.312 F- 5.765G- 7.328H+ 3.695I- 0.267J - 3.428K | 0.9406 |

A: Reaction time (min)_30; B: Reaction time (min)_40; C: Reaction time (min)_50; D: Microwave power (kW)_1.0; E: Microwave power (kW)_1.5; F: Microwave power (kW)_2.0; G: Microwave power (kW)_2.5; H: Microwave power (kW)_3.0; I: Microwave susceptor (%)_10; J: Microwave susceptor (%)_15; K: Microwave susceptor (%)_20

Results evidenced that a lower biochar yield was obtained at 3 kW at various residence times and 20% susceptor, achieving between 11.9 to 13.67 wt%. High susceptor addition and increased microwave power produce low biochar yield. These operating conditions contribute to increased heating rates and facilitate the formation of volatiles from the bagasse and the

thermal breakdown of heavy hydrocarbon, generating more liquid and gas compounds (Li et al., 2018; Sakhiya et al., 2020; Zhang et al., 2017a). However, higher M.S addition and lower power (1-1.5 kW) induced better yield (49% higher) than 3 kW. Regardless of the low pyrolysis power, higher susceptor addition enhance the microwave absorption and accelerate the biomass breakdown without exceeding the heating beyond the devolatilization of biochar (Agu et al., 2022; Kadlimatti et al., 2019; Zhang et al., 2017a). This finding is validated by some studies reported in (S & Paramasivan, 2021; Zhang et al., 2017a).

The mass loss of feedstock is generated by two factors: water loss and organic matter decomposition. In the carbonization stage, the liquid and gaseous products are produced. Both yields depend on raw biomass properties, such as volatile matter and water content (Kosakowski et al., 2020). Moreover, inorganic substances and the moisture content in the biomass have a considerable impact on the quality and yield of biochar (Mierzwa-Hersztek et al., 2019). Biomass with high water content pyrolysed using high power causes higher energy release, enhancing the decomposition and depolymerization of lignocellulosic compounds. At the same time, higher input power advances the presence of moisture in the biochar pores, reducing its heating value (Shin Ying Foong, 2020; Zhang et al., 2017a).

### 3.2.2 Bio-oil yield optimisation

Some studies reported that higher power and longer treatment time are optimal biomass treatments to achieve higher bio-oil yield (Suriapparao et al., 2015). Nevertheless, maximum operational conditions were not always desirable parameters to obtain the highest bio-oil yield, which can lead to a critical secondary breakdown of oil components into non-condensable volatiles (Kadlimatti et al., 2019; S.Mutsengerere et al., 2019; Shi et al., 2020). The results showed that the highest bio-oil yield was 25.37 wt% attained at 2 kW, 30 minutes of residence time and 10% M.S. Bio-oil yield improved when more energy was released in the conversion process generating a breakdown of the organic bonds of SCB forming liquid products (condensable gases) (Y. Zhang et al., 2017). Then, 2 kW was enough microwave power to complete the pyrolysis process and reach the optimal bio-oil temperature (Yaning Zhang, 2017). Figure 5 shows bio-oil yields from the microwave-assisted conversion process, and its respective regression equation is described in Table 4.

The increased input power and high susceptor improving the residence time to reach the heating rate, high pyrolysis temperature led to low bio-oil yield (Khelfa et al., 2020; S.Mutsengerere et al., 2019; Y. Zhang et al., 2017). This asseveration can be confirmed by

observing the variation of bio-oil performance from 2 kW to 3 kW, obtaining a reduction yield of 63%. The excess pyrolysis temperature generated by the higher microwave power or/and microwave susceptor addition involves higher temperatures beyond the optimal condition for bio-oil production, reducing the solid and liquid products but increasing gas formation (Kadlimatti et al., 2019; Yaning Zhang, 2017). Therefore, there was a higher production of low molecular weight compounds due to the second breakdown of condensable vapours into syngas generation (Yaning Zhang, 2017; Zhang et al., 2017a).

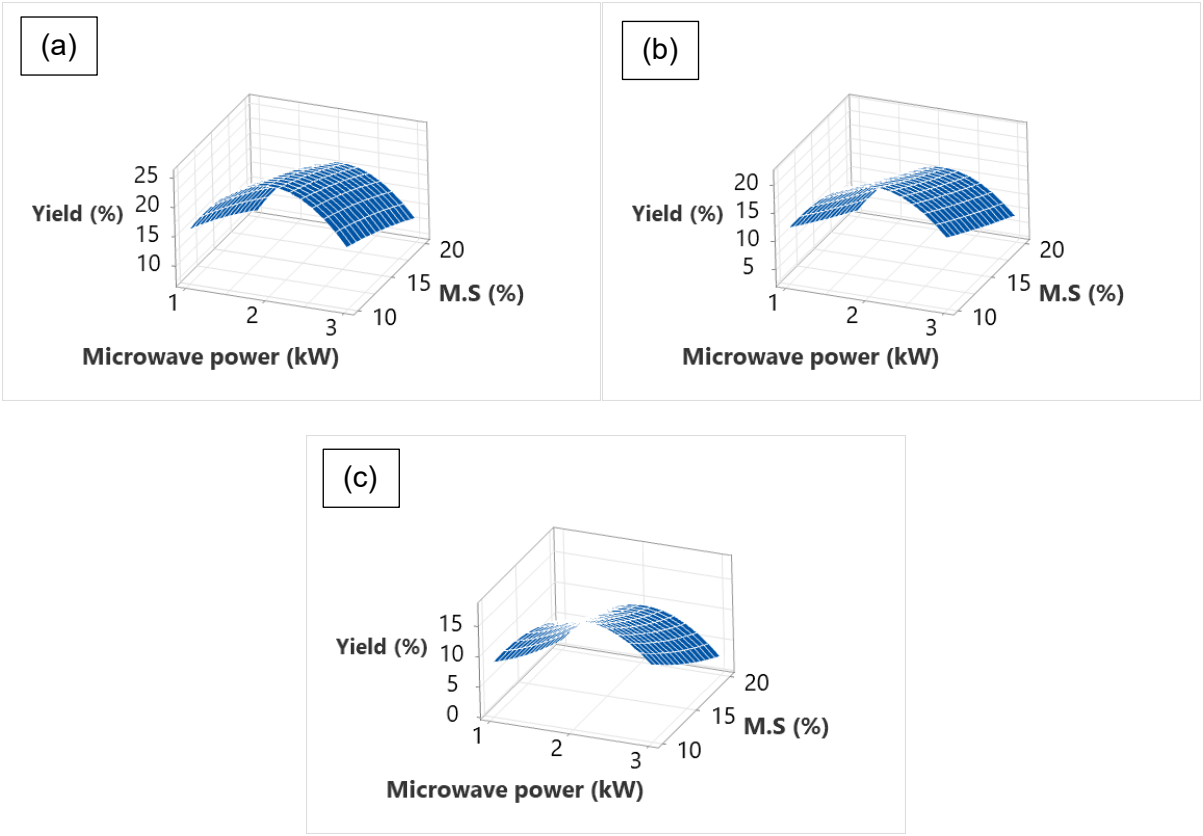


Figure 5: Response surface plot of bio-oil yield under (a) 30, (b) 40, and (c) 50 minutes of microwave pyrolysis.

Table 4: Regression equation of bio-oil yield versus reaction time, microwave power and microwave susceptor

| | R-sq (%) |
|---|---|
| B.O_Y(%)=13.450+3.946A-0.204B-3.742C-.512D+1.190E+5.331F+1.267G-2.276H+4.102I-0.082J-4.019K | 0.9729 |

A: Reaction time (min)_30; B: Reaction time (min)_40; C: Reaction time (min)_50; D: Microwave power (kW)_1.0; E: Microwave power (kW)_1.5; F: Microwave power (kW)_2.0; G:

Microwave power (kW)_2.5; H: Microwave power (kW)_3.0; I: Microwave susceptor (%)_10; J: Microwave susceptor (%)_15; K: Microwave susceptor (%)_20

The microwave susceptor produces oxygen migration from the condensable bio-oil to the non-condensable gases, inducing low bio-oil yield and high biogas production (Shi et al., 2020). The resulting optimisation showed a bio-oil yield reduction of 49% by increasing the susceptor from 10% to 20%, operating at 2 kW for 30 minutes. Moreover, an appropriate residence time is required to complete the microwave pyrolysis process and reach the optimal pyrolysis temperature, promoting the decomposition of biomass compounds (increased chemical reactions), like a breakdown of organic bonds of biomass to produce condensable gases. Increased residence time from 30 to 40 minutes and input power from 1 kW to 1.5 kW with a 10% M.S conducted to an increased bio-oil yield of 7%. However, increasing the treatment time to 50 minutes caused a decreased bio-oil yield of 18%. Longer pyrolysis time promotes organic volatile formation due to the devolatilization of biomass. An extended thermochemical decomposition reached higher pyrolysis temperatures than were desirable, causing non-condensable gas formation. Previous studies reported a critical temperature of over 550 ºC (Kadlimatti et al., 2019; Lin & W.Chen, 2015). Hence, the optimal residence time for bio-oil production varied based on diverse factors associated with input power and the susceptor ratio (Y. Zhang et al., 2017).

The moisture content of the biomass used in the microwave pyrolysis process has a crucial impact on the yield and quality of the bio-oil (Ethaib et al., 2020). High moisture content can improve the bio-oil yield. However, a significant proportion of liquid products involves light oil with a high aqueous concentration, as water and hydro-soluble compounds (Ethaib et al., 2020; Giorcelli et al., 2021; Zhang et al., 2017a). The aqueous fraction in bio-oil can be generated by chemical reactions associated with the microwave pyrolysis process (Yaning Zhang, 2017). For example, the aqueous fraction can come from the thermal decomposition of lignocellulosic compounds, low molecular weightacidsd and aldehydes (Budarin et al., 2015). Bio-oil quality is affected by the presence of water due to its low heating value (Yaning Zhang, 2017).

### 3.2.3 Biogas yield optimisation

Figure 6 shows the biogas yield distribution, and Table 5 indicates the general linear model of the biogas yield optimisation. The highest biogas yield was 84.43 wt% and 80.19 wt%. These yields were obtained at various operational parameters. The first optimisation was at 3 kW with

20% microwave susceptor for 50 minutes, achieving 84.43 wt%. The second stage involved exposing the biomass to 3 kW with 20% M.S for 40 minutes, obtaining a 76.93 wt% biogas yield. Nonetheless, the lowest yield was 51.67 wt% at 2 kW with 15% microwave susceptor for 30 minutes.

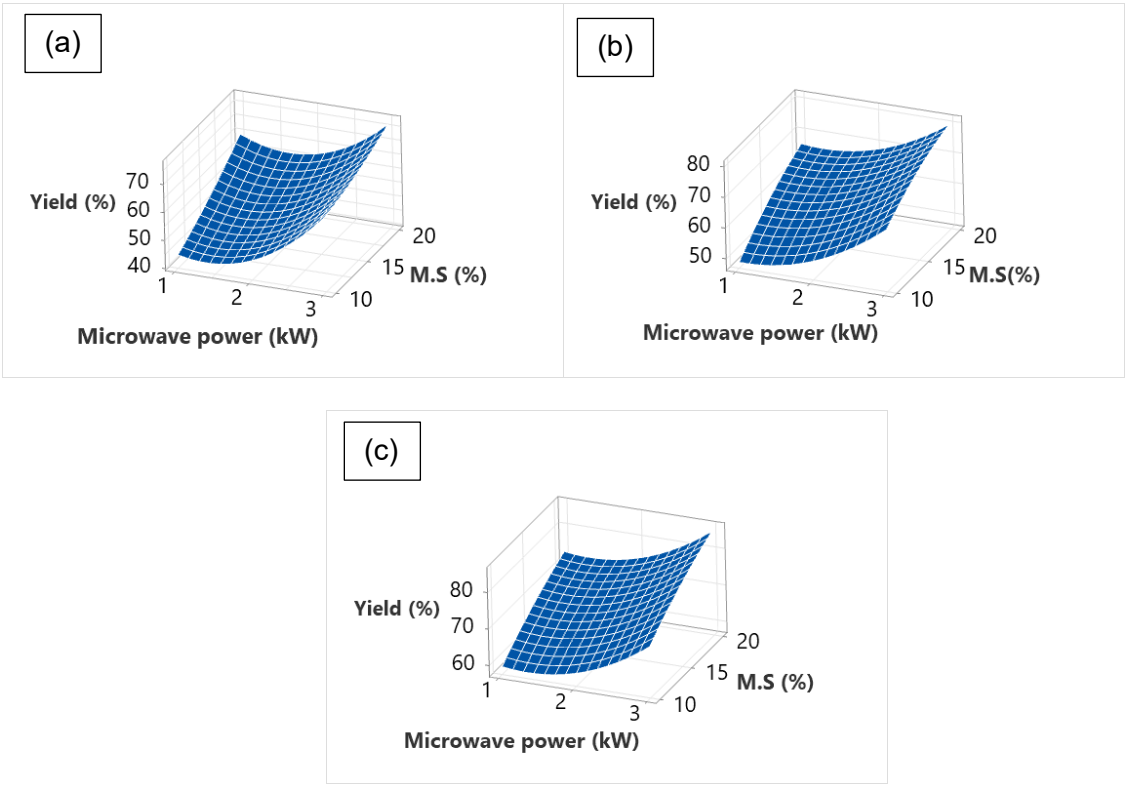


Figure 6: Response surface plot of biogas yield under (a) 30, (b) 40, and (c) 50 minutes of microwave pyrolysis.

Table 5: Regression equation of biogas yield versus reaction time, microwave power and microwave susceptor

| | R-sq (%) |
|---|---|
| B.G_Y(%)=63.865-5.852A-0.553B+6.406C-3.761D-6.323E-4.020F +4.498G +9.605H-7.796I+0.350J+7.447K | 0.9729 |

A: Reaction time (min)_30; B: Reaction time (min)_40; C: Reaction time (min)_50; D: Microwave power (kW)_1.0; E: Microwave power (kW)_1.5; F: Microwave power (kW)_2.0; G: Microwave power (kW)_2.5; H: Microwave power (kW)_3.0; I: Microwave susceptor (%)_10; J: Microwave susceptor (%)_15; K: Microwave susceptor (%)_20

The results show that time is a relevant factor in biogas yield, where the conversion process must be long enough to complete the biomass pyrolysis (Y. Zhang et al., 2017; Zhang et al., 2017a). Short treatment time and low power are not the optimal parameters to achieve a high by-product yield due to the impossibility of reaching the ideal pyrolysis temperature in a short time and the breakdown of lignocellulosic biomass compounds. In contrast, prolonged pyrolysis and high microwave power promote low molecular weight compounds, leading to secondary reactions, where condensable vapours generated in the chamber are decomposed into syngas components, increasing the biogas yield (Kadlimatti et al., 2019; Yaning Zhang, 2017). For example, the lowest biogas yield was increased by 14% when residence time was prolonged from 30 to 50 minutes, considering treatment settings of 1.5 kW and 10% susceptor.

The combination of high input power and high microwave susceptor content provokes an increased heating rate, facilitating biogas formation. High heat release induces the decomposition of heavy intermediate vapours into non-condensable gases (Kadlimatti et al., 2019; Supramono et al., 2015). The result shows that biogas yield increased by 40% when the power increased from 1 kW to 3 kW, considering 10% susceptor and 30 minutes of treatment time. Moreover, by increasing the susceptor concentration from 10% to 20%, the biogas yield increased by 34 wt% at 1 kW and 40 minutes of residence time. Another influencing factor was the moisture of the raw biomass, which promotes syngas production. Biomass water content contributes to microwave absorbance because of its high tanδ value of 0.12, generating a higher temperature increase rate in the early stage of the pyrolysis process related to water evaporation (Yaning Zhang, 2017). Therefore, the biomass moisture content can improve the volatilization process due to the breakdown of liquid products (secondary reactions), forming permanent gaseous compounds (Zhang et al., 2017a). In this case, the raw biomass applied in the experiments has no pre-drying pretreatment.

## 3.3 By-products characterisation

### 3.3.1 Biochar analysis

To better understand the effect of the microwave pyrolysis process on the biochar quality, CHNS elemental analysis was undertaken. The microwave pyrolysis parameters and ultimate analysis are shown in Table 6. The results demonstrate that a high pyrolysis power produces biochar with high carbon content and low oxygen and nitrogen presence. This phenomenon is due to the high input power, which leads to more breakdown of chemical bonds, e.g., C-O and C-H (Shin Ying Foong, 2020; Wallace et al., 2019). For example, the biochar generated at 2 kW, 10% microwave susceptor and 30 minutes of pyrolysis resulted in the highest carbon

content (57%) and the lowest oxygen concentration (39%). Unlike the biochar produced at 2 kW power, 40 minutes reaction time and 20% M.S resulted in the lowest carbon content (27%) and the highest oxygen presence (72%). A higher concentration of microwave susceptor (20%) produced higher heating rates, involving less water loss during biomass degradation. Then, a high pyrolysis temperature reached in a shorter reaction time forms more pores, trapping the moisture from the biochar (Shin Ying Foong, 2020; Tomczyk et al., 2020).

The carbonization (O/C) and aromatization(H/C) degrees were reduced using high microwave power. The lowest H/C ratio (0.01) was reached at 2 kW input power, 40 minutes of reaction time and 20% M.S. The scenario of 2 kW, 30 minutes pyrolysis time and 10% microwave susceptor achieved the lowest O/C ratio (0.68). Previous studies have reported that the O/C and H/C ratios should be less than 0.4 and 0.6, respectively (Mierzwa-Hersztek et al., 2019). Reduction of the O/C and H/C ratio is associated with the high aromaticity properties and lower polarity of the biochar generated from the microwave pyrolysis conditions (Tomczyk et al., 2020). Therefore, high microwave power promotes the carbon and thermal stability of biochar (M.Waqasa et al., 2018; Mierzwa-Hersztek et al., 2019).

Apart from biochar yield, the variation of microwave power, reaction time, and microwave susceptor also affected the heating value of the biochar due to the thermal decomposition of lignocellulosic compounds (Huang et al., 2016; Nizamuddin et al., 2018). The heating value of cellulose and hemicellulose are much lower than lignin. Therefore, the volatilization of those components in the biomass contributes to the biochar heating value. There is a higher thermal breakdown of cellulose and hemicellulose content at a low microwave power but not very much cracking of lignin components, thus increasing the biochar heating value (Huang et al., 2016). Moreover, high oxygen content causes a significant reduction in the biochar heating value, affecting its quality as fuel (Nizamuddin et al., 2018). For example, the results show that the highest biochar LHV (18.22 MJ/kg) was obtained at 2 kW power, 30 minutes of pyrolysis and 10% microwave susceptor, which also represents the highest carbon content (57.61%) and the lowest oxygen concentration (39.03%). However, 2.14 MJ/kg was the lowest heating value attained, representing only 27.23% oxygen content.

Table 6: Ultimate analysis of biochar obtained at different operational conditions

| **Microwave pyrolysis sample condition** | **N%** | **C%** | **H%** | **O*%** | **H/C** | **O/C** | **LHV (MJ/kg)** |
|---|---|---|---|---|---|---|---|

| | | | | | | | |
|---|---|---|---|---|---|---|---|
| **1.5 kW/30min/10%M.S** | 0.39 | 55.33 | 2.56 | 41.72 | 0.05 | 0.75 | 16.21 |
| **2 kW/30min/10%M.S** | 0.36 | 57.61 | 3 | 39.03 | 0.05 | 0.68 | 18.22 |
| **2 kW/30min/15%M.S** | 0.24 | 37.75 | 0.37 | 61.64 | 0.01 | 1.63 | 2.97 |
| **1 kW/30min/20%M.S** | 0.3 | 36.29 | 0.7 | 62.71 | 0.02 | 1.73 | 2.88 |
| **1 kW/40min/10%M.S** | 0.48 | 44.07 | 1.48 | 53.97 | 0.03 | 1.22 | 8.39 |
| **2 kW/40min/20%M.S** | 0.16 | 27.33 | 0.28 | 72.23 | 0.01 | 2.64 | 2.14 |
| **3 kW/30min/20%M.S** | 0.4 | 54.6 | 1.34 | 43.66 | 0.02 | 0.80 | 13.468 |

O*, oxygen was calculated employing the difference between the total percentage and all the remaining elements.

Figure 7 and Figure 8 show the combustion and thermal performance of biochar generated from different microwave pyrolysis conditions. The decomposition stability is represented in the thermogravimetric analysis (TGA) and derivative thermogravimetry (DTG). The graph shows that biochar produced at higher microwave power (2 kW) presents less weight loss at the early stage (3%), between 100-150 ºC. However, low input power (1 kW) cause slightly higher weight loss (5%). Moreover, higher power generates more weight loss at a later stage of the pyrolysis reaction than low power. A weight loss of 21% and 24% for the samples produced at 1.5 kW and 2 kW was observed at range temperatures of 350-750 ºC, respectively. The mass loss increase at high temperatures was due to the thermal decomposition of the lignin and inorganic compounds and the high moisture removal from the biochar at high pyrolysis power (Brickler et al., 2021; Nizamuddin et al., 2018). Therefore, high pyrolysis temperatures cause more thermal stability of the biochar (Mohammed et al., 2015).

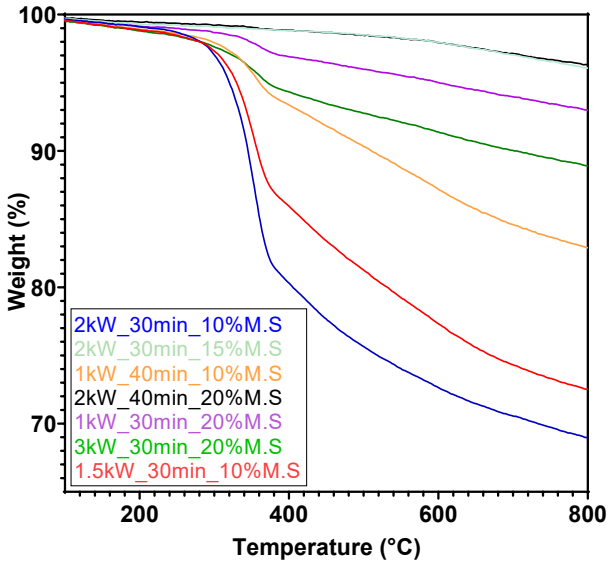

Figure 7: TGA curve of biochar generated at different microwave power, reaction time and microwave susceptor.

The DTG curve shows the difference in the thermal peak quantity of biochar. The first peak was obtained between 250 ºC to 400 ºC, which involves the degradation of cellulose and hemicellulose components. High microwave power promotes the volatilization of biochar, which is associated with dehydrogenation and aromatization (Mohammed et al., 2015). For example, there was a 94.4% difference in the thermal peak between the raw biomass and the biochar obtained at 3 kW, 30 minutes of pyrolysis and 20% microwave susceptor. However, 2 kW and 10% microwave susceptor achieved only 59% volatilization.

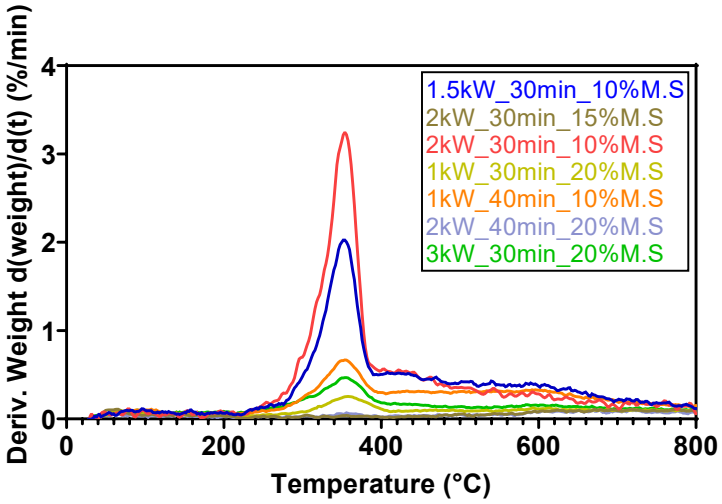


Figure 8: DTG curve of biochar generated at different microwave power, reaction time and microwave susceptor.

The structural porosity and morphology of biochar generated from microwave pyrolysis have a higher surface area and pore volume (Leng et al., 2021). Figure 9 shows the SEM image of sugarcane bagasse biochar at different microwave operational conditions. Figures 9 (a) and (c) demonstrate that the biochar produced at high pyrolysis power presents lower pore breakdown due to the quick release of volatiles during the increased heating rates. The biochar samples generated at over 1.5 kW have a small pore size, higher pore volume, higher externally accessible surface area and higher mass loss (Brickler et al., 2021; Nizamuddin et al., 2018; Tomczyk et al., 2020; Wallace et al., 2019). Moreover, high input power allows more energy production due to the breakdown of C-O bonds, generating the fragmentation, depolymerization, and decomposition of organic matter associated with lignocellulosic biomass (Shin Ying Foong, 2020). Figure 9 (b) reveals that low microwave power caused a

gradual thermal decomposition of biomass, reducing the blocking of pore formation and decreasing the mass loss (Shin Ying Foong, 2020; Wallace et al., 2019).

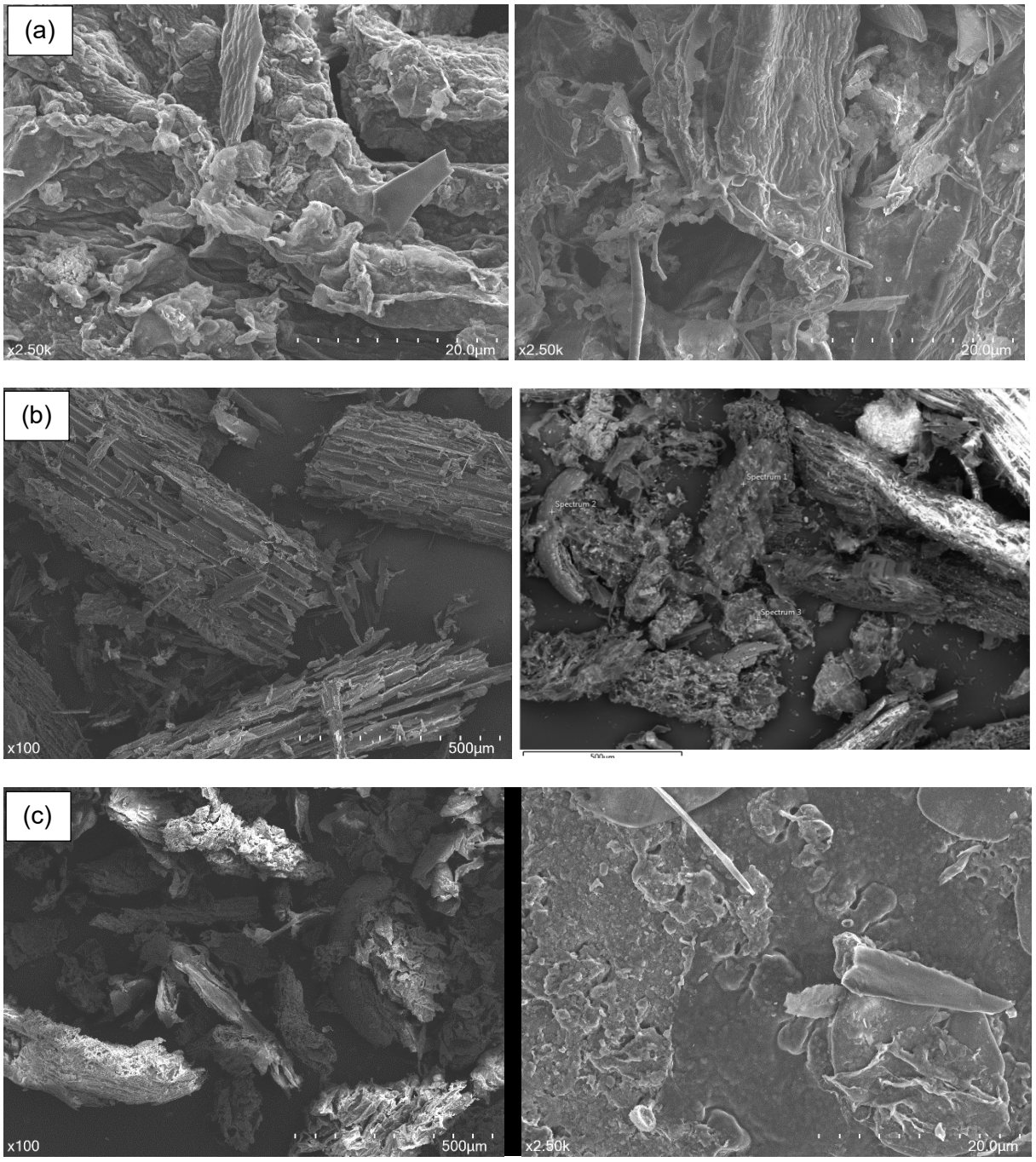


Figure 9: Scanning Electron Microscope (SEM) images of sugarcane bagasse biochar, generated at (a) 1.5 kW for 30 minutes and 10% microwave susceptor; (b) 1 kW for 40 minutes and 10% microwave susceptor; (c) 2 kW for 30 minutes and 10% microwave susceptor.

Diverse studies have reported that biochar, generated from microwave pyrolysis, presents a higher BET surface area and pore volume than conventional pyrolysis (Selvam S & Paramasivan, 2022; Suriapparao et al., 2022). Those properties determine the biochar quality for a combustion process (Halim & Swithenbank, 2016; Li et al., 2016; Sieng-Huat Kong; Su Shiung Lam; Peter Nai Yuh Yek; Rock Keey Liew; Nyuk Ling Ma; Mohammad Shahril Osman; Chee Chung Wong, 2018; Wallace et al., 2019). Table 7 indicates the surface area properties of the biochar optimisation. Results show that high microwave power and longer treatment time are the optimal conditions for obtaining a higher BET surface area, adsorption efficiency and micropore volume. For example, the surface area improved by 74% (cases BCa and BCc) when the microwave power and the microwave susceptor increased from 1.5 kW to 2 kW and 10% to 15%, respectively.

Higher power leads to a structural modification of the biochar pores due to the high volatilization of larger molecules and the rapid release of small molecules (volatile matter) generated by the increased pyrolysis temperature (Halim & Swithenbank, 2016; Li et al., 2016). For instance, high lignin decomposition promotes the quick release of $H_2$ and $CH_4$ and aromatic condensation. These conditions result in better surface pore formation during microwave pyrolysis (Mierzwa-Hersztek et al., 2019; Tomczyk et al., 2020). On the other hand, the increment of microwave susceptor and treatment time promote higher heat energy, releasing more volatiles from the surface of the sugarcane bagasse, and increasing the area and volume of the biochar. This characteristic is related to the fragmentation, depolymerization and cracking of lignocellulosic compounds (Shin Ying Foong, 2020; Zhang et al., 2017a). Higher pyrolysis heat energy leads to higher carbon stability (M.Waqasa et al., 2018). The surface area increased by 3% when the treatment time was incremented by 10 minutes (cases BCe and BCd). Then, the BET surface area improved by 62% when the microwave susceptor increased from 10% to 20% (cases BCa and BCd).

A low BET surface area is produced when biomass presents a high content of inorganic compounds, which can block the micropores in the biochar surface (Tomczyk et al., 2020). Another factor in the surface area reduction is elevated power, which can lead to excessive pyrolysis temperature, generating destruction in the biochar structure. In terms of morphologies, the biochar has agglomerates of hexagonal prism-shaped (rough surface) (Halim & Swithenbank, 2016; Shin Ying Foong, 2020). The work reported by (Leng et al., 2021) affirmed that if the temperature is not high enough (above 400 °C), the pyrolysis process won't be completed, reducing the volatile generation and pore formation. For example, sample BCb

obtained the lowest surface area (11.23 $m^2$/g) due to short pyrolysis time and low microwave susceptor were insufficient to cause the release of volatiles.

| **Analysis** | **BCa** | **BCb** | **BCc** | **BCd** | **BCe** | **BCf** | **BCg** |
|---|---|---|---|---|---|---|---|
| **Surface area (m2/g)** | | | | | | | |
| BET Surface Area | 121.78 | 11.23 | 211.60 | 197.03 | 202.16 | 157.29 | 139.29 |
| t-Plot Micropore Area | 65.03 | | 140.46 | 126.38 | 136.56 | 94.36 | 67.94 |
| t-Plot external surface area | 56.76 | 14.65 | 71.13 | 70.65 | 65.60 | 62.92 | 71.34 |
| BJH Adsorption cumulative surface area of pores | 25.24 | 8.93 | 31.79 | 31.12 | 26.03 | 35.23 | 18.95 |
| | | | | | | | |
| **Pore volume (cm3/g)** | | | | | | | |
| t-Plot micropore volume | 0.03 | 0.00 | 0.06 | 0.05 | 0.05 | 0.04 | 0.03 |
| Total pore volume calculated at p/p°<1.0228 | 0.04 | 0.00 | 0.07 | 0.06 | 0.07 | 0.05 | 0.04 |

Table 7: BET data of biochar obtained at different operational conditions

| **Analysis** | **BCa** | **BCb** | **BCc** | **BCd** | **BCe** | **BCf** | **BCg** |
|---|---|---|---|---|---|---|---|
| **Surface area ($m^2$/g)** | | | | | | | |
| BET Surface Area | 121.78 | 11.23 | 211.60 | 197.03 | 202.16 | 157.29 | 139.29 |
| t-Plot micropore Area | 65.03 | | 140.46 | 126.38 | 136.56 | 94.36 | 67.94 |
| t-Plot external surface area | 56.76 | 14.65 | 71.13 | 70.65 | 65.60 | 62.92 | 71.34 |
| BJH Adsorption cumulative surface area of pores | 25.24 | 8.93 | 31.79 | 31.12 | 26.03 | 35.23 | 18.95 |
| | | | | | | | |
| **Pore volume ($cm^3$/g)** | | | | | | | |
| t-Plot micropore volume | 0.03 | 0.00 | 0.06 | 0.05 | 0.05 | 0.04 | 0.03 |
| Total pore volume calculated <1.0228nm | 0.04 | 0.00 | 0.07 | 0.06 | 0.07 | 0.05 | 0.04 |

BCa: Biochar generated at 1.5 kW/30min/10%M.S; BCb: Biochar generated at 2 kW/30min/10%M.S; BCc: Biochar generated at 2 kW/30min/15%M.S; BCd: Biochar generated at 1 kW/30min/20%M.S; BCe: Biochar generated at 1 kW/40min/10%M.S; BCf: Biochar generated at 2 kW/40min/20%M.S; BCg: Biochar generated at 3 kW/30min/20%M.S.

### 3.3.2 Bio-oil analysis

Table 8 shows the elemental components of bio-oil produced at different microwave power, reaction time and microwave susceptor (M.S) combinations. The results show a variation in carbon, oxygen and hydrogen content based on the increment of the microwave operational conditions. For instance, the lowest oxygen content (34.41%) was obtained at 2 kW, 40 minutes of pyrolysis and 20% microwave susceptor. However, the highest oxygen content (42.59%) was produced at 1 kW, 30 minutes of pyrolysis and 20% susceptor. The main reason for this phenomenon is the deoxygenation reaction of the raw biomass generated at high microwave power, which reduces the number of functional groups during pyrolysis (Ferrera-Lorenzo et al., 2014). At the same time, a higher H/C value was achieved with lower microwave power and reaction time, involving an increase in the aliphatic group due to the decrease in microwave heating. In contrast, a lower H/C ratio was obtained with higher microwave power, higher reaction time and microwave susceptor, whose effects in bio-oil resulted in higher aromatic content (Halim & Swithenbank, 2016).

Table 8: Ultimate analysis of bio-oil obtained at different operational conditions

| **Microwave pyrolysis sample condition** | **N%** | **C%** | **H%** | **O*%** | **H/C** | **O/C** | **LHV (MJ/kg)** |
|---|---|---|---|---|---|---|---|
| **1.5kW/30min/10%M.S** | 0.33 | 55.25 | 5.88 | 38.54 | 9.40 | 0.70 | 29.89 |
| **2kW/30min/10%M.S** | 0.44 | 55.46 | 6.11 | 37.99 | 9.08 | 0.68 | 30.20 |
| **2kW/30min/15%M.S** | 0.56 | 53.48 | 5.92 | 40.04 | 9.03 | 0.75 | 29.50 |
| **1kW/30min/20%M.S** | 0.42 | 51.39 | 5.60 | 42.59 | 9.18 | 0.83 | 28.63 |
| **1kW/40min/10%M.S** | 0.35 | 55.03 | 6.10 | 38.52 | 9.02 | 0.70 | 30.09 |
| **2kW/40min/20%M.S** | 0.45 | 57.73 | 7.41 | 34.41 | 7.79 | 0.60 | 32.24 |

O*, oxygen was calculated employing the difference between the total percentage and all the remaining elements.

The heating value of bio-oil is directly associated with the elemental composition of bio-oil. Decreasing the oxygen concentration cause increases its heating value due to the chemical reaction related to ketones and aldehyde concentrations. 32.24 MJ/kg was the highest heating value achieved at the lowest oxygen content. High oxygen concentration is associated with chemical instability, storage permanence, acidity, and immiscibility property of the bio-oil (Panwar & Paul, 2021; Si et al., 2017).

The elemental analysis can be contrasted by the bio-oil functional groups shown in Table 9 and Table 10. The bio-oil composition involves carboxylic acid, ketones, aromatic, sugar, phenols, guaiacol, alkanes, alkynes, and alcohol. Microwave pyrolysis produces more phenol compounds due to higher condensation temperature at the early stage (Zhao et al., 2021). Results show that the concentration of phenol groups is 33% higher in bio-oil samples produced at 1 kW than at 2 kW. The combination of lower power and higher addition of susceptor allowed reaching a higher pyrolysis temperature, leading to the cracking of lignin compounds to the conversion into phenol groups. Hence, higher microwave power leads to the breakdown of phenols, reducing their concentration (Mohammed et al., 2015; Zhao et al., 2021). High phenol content is associated with a higher H/C ratio (Halim & Swithenbank, 2016).

Lower microwave power produces slightly higher aromatic content (10%) due to the higher pyrolysis temperature leading to the breakdown of aromatics, generating more phenol groups (Lyu et al., 2015). The concentration of aromatic groups is related to a high heating value and bio-oil quality because of the low concentration of oxygenated compounds (Khuenkaeo et al., 2021). On the other hand, 2 kW achieved more concentration of sugars (61.23%), ketones (2.49%), and carboxyl acid (8.37%). The higher sugar content is due to the breakdown of cellulose compounds generated with higher microwave power. For example, alpha-D-Glucopyranose, 1,6-anhydro- (49.75%) is associated with the feedstock type (Lyu et al., 2015; Zhang & Xiong, 2016). Since the pyrolytic sugar has water-solubility properties, it can be removed from the bio-oil by applying some liquid-liquid extraction method. Furthermore, the pyrolytic sugar is extracted from bio-oil to convert it into fuels, and by using phenols, it is possible to obtain chemical products, like green diesel and adhesives (Rover, 2013; Yu et al., 2016).

Ketone groups are generated by the decomposition of hemicellulose (from hexoses) and cellulose compounds. The study reported by (Lyu et al., 2015) established that a high concentration of metal ions can produce a secondary reaction of sugar compounds like

levoglucosan and generate ketones. The ketones concentrations increased by 2.5% when the microwave power increased to 2 kW. This phenomenon is explained by the ketonization reaction, which means that two carboxylic acids are converted into a ketone, carbon dioxide and water by applying higher heat (higher power) (Pham et al., 2013; Wang et al., 2018). At the same time, increased microwave power produced slightly higher carboxylic acid content (37%) which can represent higher oxygen content, a reduction of storage stability, and increased corrosiveness (Ferrera-Lorenzo et al., 2014; Panwar & Paul, 2021; Si et al., 2017; Wang et al., 2012). Higher carboxylic acid concentration can increase the polarity of bio-oil, involving higher solubility in other polar solvents (Rover, 2013).

Table 9: Distribution of chemical compounds of bio-oil generated at 1 kW during 30 minutes of microwave pyrolysis and 20% M.S

| **Classification** | **Compound** | **Concentration (microgram/gram)** | **Concentration (%)** |
|---|---|---|---|
| **Carboxylic acid** | Acetic acid, methyl ester | 673 | 1.54 |
| | Acetic acid | 1641 | 3.76 |
| | | | **5.30** |
| **Ketone** | 2-Butanone | 149 | 0.34 |
| | Benzaldehyde, 4-hydroxy- | 380 | 0.87 |
| | | | **1.21** |
| **Phenols** | Phenol | 552 | 1.26 |
| | Phenol, 3-methyl- | 931 | 2.13 |
| | Phenol, 2,6-dimethyl- | 216 | 0.49 |
| | Creosol | 752 | 1.72 |
| | Phenol, 4-ethyl- | 1623 | 3.72 |
| | 2-Allylphenol | 349 | 0.80 |
| | 3,5-Dimethoxy-4-hydroxytoluene | 1517 | 3.47 |
| | Benzaldehyde, 3-hydroxy-4-methoxy- | 1406 | 3.22 |

| | | | |
|---|---|---|---|
| | 5-tert-Butylpyrogallol | 380 | 0.87 |
| | | | **17.69** |
| **Guaiacol** | 2-Methoxy-4-vinylphenol | 126 | 0.29 |
| | Phenol, 2-methoxy-4-(1-propenyl)- | 522 | 1.20 |
| | Phenol, 2,6-dimethoxy- | 2083 | 4.77 |
| | Phenol, 2,6-dimethoxy-4-(2-propenyl)- | 420 | 0.96 |
| | Phenol, 2,6-dimethoxy-4-(2-propenyl)- | 321 | 0.73 |
| | | | **7.95** |
| **Alkanes** | Undecane | 370 | 0.85 |
| | Heptane, 2,2,4,6,6-pentamethyl- | 1909 | 4.37 |
| | Cyclotrisiloxane, hexamethyl- | 106 | 0.24 |
| | | | **5.46** |
| **Alkynes** | Methylcodeine | 728 | 1.67 |
| | | | **1.67** |
| **Alcohols** | Silane, trimethoxymethyl- | 89 | 0.20 |
| | 1-(2-Acetoxyethyl)-3,6-diazahomoadamantan-9-one oxime | 322 | 0.74 |
| | Cyclopropyl carbinol | 300 | 0.69 |
| | | | **1.63** |
| **Aromatic** | Toluene | 274 | 0.63 |
| | Benzofuran, 2,3-dihydro- | 2330 | 5.33 |
| | | | **5.96** |
| | 2,3-Anhydro-d-galactosan | 1670 | 3.82 |
| | Aminocarb | 664 | 1.52 |

| | | | |
|---|---|---|---|
| **Sugars** | Apocynin | 401 | 0.92 |
| | Triacetyl-d-mannosan | 2791 | 6.39 |
| | 1,3-Di-O-acetyl-à-á-d-ribopyranose | 1027 | 2.35 |
| | Alpha-D-Glucopyranose, 1,6-anhydro- | 16659 | 38.14 |
| | | | **53.14** |

Table 10: Distribution of chemical compounds of bio-oil generated at 2 kW during 30 minutes of microwave pyrolysis and 10% M.S

| **Classification** | **Compound** | **Concentration (microgram/gram)** | **Concentration (%)** |
|---|---|---|---|
| **Carboxylic acid** | Acetic acid, methyl ester | 832 | 0.83 |
| | Acetic acid | 2130 | 2.13 |
| | Hexanoic acid, 2-ethyl- | 673 | 0.67 |
| | 3-Isoxazolecarboperoxoic acid, 4,5-dihydro-5-phenyl-, 1,1- | 751 | 0.75 |
| | o-Ethylhydroxylamine | 3971 | 3.98 |
| | | | **8.37** |
| **Ketone** | 2-Butanone | 156 | 0.16 |
| | 2-Methyliminoperhydro-1,3-oxazine | 1057 | 1.06 |
| | 4-Methyl-2-oxopentanenitrile | 1277 | 1.28 |
| | | | **2.49** |
| | Phenol | 1169 | 1.17 |
| | Creosol | 1488 | 1.49 |
| | Phenol, 3-methyl- | 681 | 0.68 |

| | | | |
|---|---|---|---|
| **Phenols** | Phenol, 2,6-dimethyl- | 463 | 0.46 |
| | Phenol, 4-ethyl- | 2648 | 2.65 |
| | Phenol, 4-ethyl-3-methyl- | 618 | 0.62 |
| | 1,2-Benzenediol, 3-methoxy- | 743 | 0.74 |
| | 3,5-Dimethoxy-4-hydroxytoluene | 2153 | 2.16 |
| | Benzaldehyde, 3-hydroxy-4-methoxy- | 1819 | 1.82 |
| | 5-tert-Butylpyrogallol | 623 | 0.62 |
| | Benzaldehyde, 4-hydroxy- | 896 | 0.90 |
| | | | **13.32** |
| **Guaiacol** | Phenol, 2,6-dimethoxy-4-(2-propenyl)- | 1376 | 1.38 |
| | Phenol, 2-methoxy- | 544 | 0.54 |
| | 2-Methoxy-4-vinylphenol | 561 | 0.56 |
| | Phenol, 2,6-dimethoxy- | 3281 | 3.29 |
| | | | **5.77** |
| **Aromatic** | Benzofuran, 2,3-dihydro- | 5370 | 5.38 |
| | | | **5.38** |
| **Alkanes** | Heptane, 2,2,4,6,6-pentamethyl- | 660 | 0.66 |
| | Alpha-Hydroxyquebrachamine | 607 | 0.61 |
| | | | **1.27** |
| **Alcohols** | 1-Decanol, 2-hexyl- | 715 | 0.72 |
| | Silane, trimethoxymethyl- | 318 | 0.32 |
| | Cyclopropyl carbinol | 1126 | 1.13 |

| | | | |
|---|---|---|---|
| | | | **2.16** |
| **Sugars** | 1,3-Di-O-acetyl-à-á-d-ribopyranose | 1434 | 1.44 |
| | Aminocarb | 876 | 0.88 |
| | Triacetyl-d-mannosan | 5715 | 5.72 |
| | Apocynin | 587 | 0.59 |
| | Alpha-D-Glucopyranose, 1,6-anhydro- | 49663 | 49.75 |
| | 2,3-Anhydro-d-galactosan | 2849 | 2.85 |
| | | | **61.23** |

Figure 10 and Figure 11 show the thermogravimetric analysis (TGA) and derivative thermogravimetry analysis (DTG). The results did not show much variation in the thermal deformation between the different bio-oil samples. The initial thermal decomposition happens between 250°C and 350°C, which involves moisture evaporation and highly volatile compounds. Also, at that temperature range, hemicellulose degradation occurs (Armando T. Quitain, 2015). The bio-oil generated at 2 kW for 30 minutes and 10% microwave susceptor resulted in around 39% weight loss. Differently, the weight reduction of the bio-oil produced at 1 kW for 30 minutes and 20% microwave susceptor was 24%. The rapid thermal degradation is generated by the volatilization of residual solvent (alcohols), water and light components (Sainab Omar, 2019; Suzanne Anouti, 2016). The last thermal decomposition is between 400°C and 600°C conducted by the breakdown of heavy compounds, stability, and lignin degradation (Armando T. Quitain, 2015).

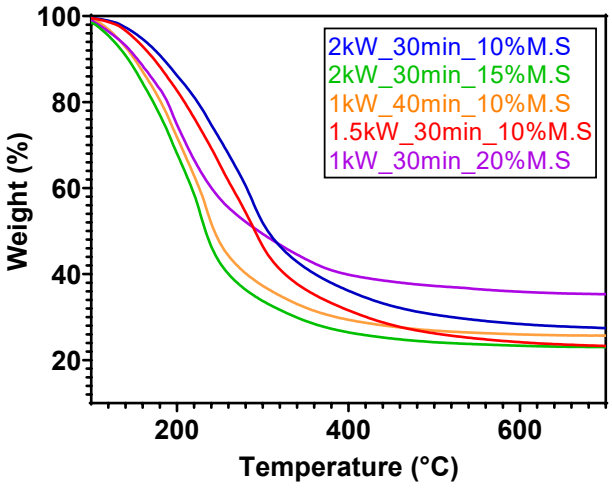

Figure 10: TGA curve of bio-oil generated at different microwave power, reaction time and microwave susceptor.

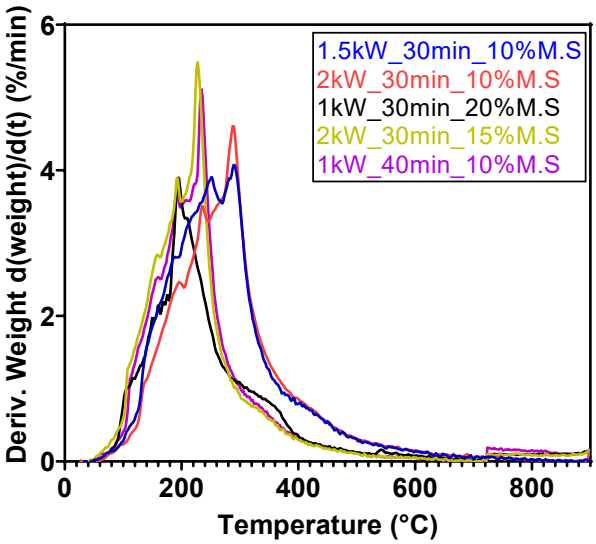


Figure 11: DTG curve of bio-oil generated at different microwave power, reaction time and microwave susceptor.

### 3.3.3 Biogas analysis

Through Gas Chromatograph (Shimadzu GC 2030), it was possible to determine biogas compounds obtained under various operational conditions. Table 11 shows the energy values of sugarcane bagasse gas obtained in the pyrolysis process. The biogas yield is directly relative to its heating value due to a higher yield achieved when the secondary breakdown of non-condensable volatiles occurs, increasing the formation of $H_2$, CO and $CH_4$. This phenomenon is relative to the self-gasification of the biochar during the high pyrolysis power (Lin & W.Chen, 2015; Shi et al., 2020; Zhang et al., 2017a).

The heating value was calculated considering the $H_2$, CO and $CH_4$ formation. Higher methane formation and energy value are obtained using higher microwave power, longer pyrolysis time and higher microwave susceptor. For instance, the biogas heating value generated at 1 kW for 30 minutes was 55% lower than the biogas produced at 2 kW for 40 minutes. Increased microwave power leads to a quicker microwave absorbance capacity of the biochar and thermochemical reaction. The high presence of a carbon microwave susceptor could produce elevated $CO_2$ due to the thermal decomposition of methane gas and light hydrocarbons (Shi et al., 2020). The biogas impurities comprise the $H_2S$ gas associated with the sulphuric and

nitrogen content in the formation of pyrolysis gas and its presence in the lignocellulosic biomass (Juan Camilo Solarte-Toro, 2018).

Table 11: Composition and low heating value of six biogas samples at different pyrolysis conditions

| Operational conditions | $CO_2$ (% Mol) | $CH_4$ (% Mol) | $H_2S$ (%Mol) | $O_2$ (%Mol) | $N_2$ (%Mol) | LHV (MJ/kg) |
|---|---|---|---|---|---|---|
| **1.5kW/30min/10%M.S** | 2.81 | 0.70 | 0.08 | 17.32 | 78.59 | 0.251 |
| **1kW/40min/10%M.S** | 2.12 | 0.57 | 0.05 | 17.37 | 79.39 | 0.206 |
| **2kW/30min/10%M.S** | 3.86 | 1.24 | 0.19 | 7.54 | 86.65 | 0.445 |
| **2kW/30min/15%M.S** | 2.07 | 0.84 | 0.07 | 18.10 | 78.22 | 0.302 |
| **1kW/30min/20%M.S** | 2.19 | 0.66 | 0.09 | 17.81 | 79.24 | 0.237 |
| **2kW/40min/20%M.S** | 6.89 | 1.47 | 0.28 | 12.78 | 78.04 | 0.528 |

### 3.4 Energy balance of microwave pyrolysis process

The output energy of the by-products was calculated considering their heating value, yield and biomass weight. Table 12 shows that the highest total output energy (0.24 kWh) was obtained at 2 kW, 30 minutes of pyrolysis and 10% of microwave susceptor. Mainly, this performance was obtained by the high yield and heating value of bio-oil (0.498 MJ/kg). In contrast, the output energy in by-products generated at 1 kW and 10% M.S was 95% lower than samples produced at 2 kW and 20% M.S. Low pyrolysis power, short treatment time and high microwave susceptor are not the optimal combination to achieve the energy by-products. These operating conditions were insufficient to reach the pyrolysis temperature and complete the thermochemical conversion of lignocellulosic compounds into biochar, bio-oil and biogas.

Table 12: Recovered energy of sugarcane bagasse by-products using microwave pyrolysis for 65g of SCB

| By-product optimised | Operational conditions | By-product energy (kWh) | | | Total output energy (kWh) |
|---|---|---|---|---|---|
| | | Char | Oil | Gas | |
| **Biochar** | 1.5kW/30min/10%M.S | 0.111 | 0.119 | 0.002 | 0.23 |
| | 1kW/40min/10%M.S | 0.058 | 0.068 | 0.002 | 0.13 |

| | | | | | |
|---|---|---|---|---|---|
| **Bio-oil** | 2kW/30min/10%M.S | 0.096 | 0.138 | 0.004 | 0.24 |
| | 2kW/30min/15%M.S | 0.012 | 0.129 | 0.003 | 0.14 |
| **Biogas** | 1kW/30min/20%M.S | 0.014 | 0.033 | 0.003 | 0.05 |
| | 2kW/40min/20%M.S | 0.007 | 0.083 | 0.006 | 0.1 |

The electrical consumption of the microwave pyrolysis system was calculated considering the input power, treatment time, and 80% electrical efficiency conversion of the microwave pyrolysis process. On the other hand, the biomass energy was obtained by the heating value of the SCB and the sample weight (65 grams). The total input energy was calculated assuming the energy supplied by the microwave system and the biomass. Table 13 shows the different energy recovery values obtained from the optimisation process. The results showed a significant energy difference between the operating combinations of the microwave system. The energy conversion efficiency for the samples generated at 1 kW/30min/20%M.S and 2 kW/40min/20%M.S were 74% and 70% lower than the setting scenario of 1.5 kW for 30 minutes and 10% M.S, respectively. In this way, a longer treatment time or low input power is not necessarily convenient for reaching higher energy efficiency. It is important to note that this optimal operational energy condition is relative to the required quality of each by-product. For example, a higher biochar quality is achieved using low power and longer treatment time, but better bio-oil properties (HHV, oxygen content, and aromatic functional groups) are developed at higher power and longer pyrolysis time.

Table 13: Energy recovery efficiency of microwave pyrolysis system

| B.O* | Microwave power, kW | Time, min | E.E** kWh/kg | Electrical consump. kWh | Biomass energy, kWh | Total input energy kWh | Energy conversion effic % |
|---|---|---|---|---|---|---|---|
| **Biochar** | 1.5 | 30 | 0.8 | 0.9 | 0.9 | 1.8 | 12.6 |
| | 1 | 40 | 0.7 | 0.8 | | 1.7 | 7.4 |
| **Bio-oil** | 2 | 30 | 1.0 | 1.3 | | 2.2 | 11.1 |
| | 2 | 30 | 1.0 | 1.3 | | 2.2 | 6.7 |
| **Biogas** | 1 | 30 | 0.5 | 0.6 | | 1.5 | 3.3 |
| | 2 | 40 | 1.3 | 1.7 | | 2.6 | 3.8 |

*B.O: By-product optimised

** E. E: Energy expended during the microwave pyrolysis of SCB, considering microwave power and treatment time

The output energy of the by-products showed that biomass exposed at 2 kW for 30 minutes and 10**%** microwave susceptor obtained the highest output energy (0.24 kWh**),** with bio-oil representing 68% of the total energy value. The bio-oil quality analysis showed that increasing pyrolysis temperature increased ketones functional groups concentration by up to 2.5%, improving its quality. The highest biochar output energy was obtained at 1.5kW/30min/10%M.S, considering 37.16% yield, 0.21 MJ/kg LHV, 55.33% carbon and 41.72% oxygen content. The same setting operating parameters achieved optimal energy recovery (12.6%).

### 3.5 Economic analysis

The economic analysis is based on the lab-scale microwave pyrolysis system. Table 14 shows the economic analysis of the microwave pyrolysis system. Some operating costs are feedstock, electricity purchased, microwave susceptor and maintenance (0.23 AUD/day) (Lam et al., 2019). The incurred cost of feedstock and microwave susceptor (M.S) was free because agricultural waste was used as biomass, and biochar produced in the pyrolysis process was utilised as M.S. The average electricity usage rate in Queensland is 20.19 c/kWh (Mullane, 2022). The unit values generated from the by-products are 0.55 AUD/kg biochar (Wang et al., 2015), 1.45 AUD/L bio-oil (Inayat et al., 2022; Wang et al., 2015), and 0.099 AUD/kWh biogas (Wattanasilp et al., 2021). The economic analysis was estimated considering 975 grams of biomass and the highest and lowest energy recovery obtained from the pyrolysis process. The economic balance shows that the income generated at 1 kW was 88% lower than 1.5 kW pyrolysis power. High-income capacity is associated with the high energy generation of bio-oil (1.8 kWh) and biochar (1.67 kWh). Then, an acceptable utility cost is reached at 1.5 kW, which a total income was $1.28. The microwave pyrolysis system has economic viability and the potential to scale up the energy generation of by-products at low-cost production. Microwave pyrolysis optimisation leads the sustainable development due to its energy efficiency and economic balance (Inayat et al., 2022).

Table 14: Techno-economic analysis of the microwave pyrolysis system for 975 grams of biomass

| | **1.5kW/30min/10%M.S** | | | **1 kW/30min/20%M.S** | | |
|---|---|---|---|---|---|---|
| **Item** | **Energy (kWh)** | **Value/unit** | **Amount (AUD)** | **Energy (kWh)** | **Value/unit** | **Amount (AUD)** |

| | | | | | | |
|---|---|---|---|---|---|---|
| Feedstock | - | - | - | - | - | - |
| Microwave susceptor | - | - | - | - | - | - |
| Electricity consumed | 0.9 | 20.19, (c/kWh) | 0.18 | 0.6 | 20.19, (c/kWh) | 0.12 |
| Maintenance | | | 0.03 | | | 0.02 |
| **Total operating cost** | | | **0.21** | | | **0.14** |
| | | | | | | |
| **Item** | Energy (kWh) | Value/unit | Amount (AUD) | Energy (kWh) | Value/unit, $/kWh | Amount (AUD) |
| Biochar, AUD/kg | 1.67 | 0.55 | 0.89 | 0.21 | 0.55 | 0.11 |
| Bio-oil, AUD/L | 1.8 | 1.45 | 0.39 | 0.495 | 1.45 | 0.04 |
| Biogas, AUD/kWh | 0.03 | 0.099 | 0.03 | 0.045 | 0.099 | 0.004 |
| **Total income $** | | | **1.28** | | | **0.15** |
| **Total energy gained kWh** | **2.58** | | | **0.15** | | |
| **Total $ gained** | | | **1.07** | | | **-0.01** |

The economic analysis indicated that the total income decreased by 88% when operating conditions changed from 1.5kW/30min/10%MS to 1kW/30min/20%MS. Therefore, the microwave pyrolysis system has the potential to scale up the energy generation of by-products at low-cost production.

### 3.6 Carbon footprint analysis

GHGs emissions depend on biomass management and energy generation method. Table 15 shows a $CO_2$ emissions estimation for two different biomass management scenarios and a commonly used method for electricity generation. The evaluation was calculated considering the total biomass used during the experimental phase (65 grams) and the highest energy output provided by the by-products at 1.5kW/30min/10%M.S. Production of 0.23 kWh, using a coal-based thermal power plant produces 0.314 kg $CO_2$, considering a factor of 1.57 kg

$CO_2$/kWh (Fodah & Abdelwahab, 2022). Biomass management as stored waste (landfilling) causes the release of 0.004 kg$CO_2$, as the emission factor of raw feedstock is 57 kg $CO_2$/tonne (Cheng et al., 2020). The emission factor for burning 1 kg of biomass is 1.5 kg $CO_2$ (Fodah et al., 2021), releasing 0.1 kg $CO_2$ for the indicated sample.

Table 15*:* Life cycle impact of biomass management and energy generation methods

| The energy supplied (kWh) | Biomass (kg) | Biomass as residues kg_$CO_2$ | Incineration kg_$CO_2$ | Power plant kg_$CO_2$ |
|---|---|---|---|---|
| 0.23 | 0.065 | 0.004 | 0.1 | 0.314 |

The environmental impact can be prevented by converting biomass into valuable products using microwave pyrolysis. Unlike bio-oil and biogas, biochar has the potential for carbon capture (Mong et al., 2022). Liquid and gaseous by-products are used as biofuels for heat and electricity production. These approaches are not carbon capture methods (Huang et al., 2015; Mong et al., 2022). However, biochar works as an absorbent for carbon dioxide sequestration due to its affinity to $CO_2$ (Huang et al., 2015). Figure 12 shows the balance of $CO_2$ adsorption capacity of by-products obtained at 1.5 kW for 30 minutes and 10% M.S. The $CO_2$ adsorption capacity of biochar was 47.9 $CO_2$ eq $kg^{-1}$, whose value was calculated by Equation $(1)$. The evaluation of the carbon sequestration of the microwave pyrolysis conversion consists of 37.9% biochar yield $(B.Y)$ and 43.1% fixed carbon content $(\mathrm{FC})$.

$$(1)\ CO_2\ reduction\ potential = B.Y * FC * (\frac{80}{100}) * (\frac{44}{12})$$ (Venkatesh et al., 2022)

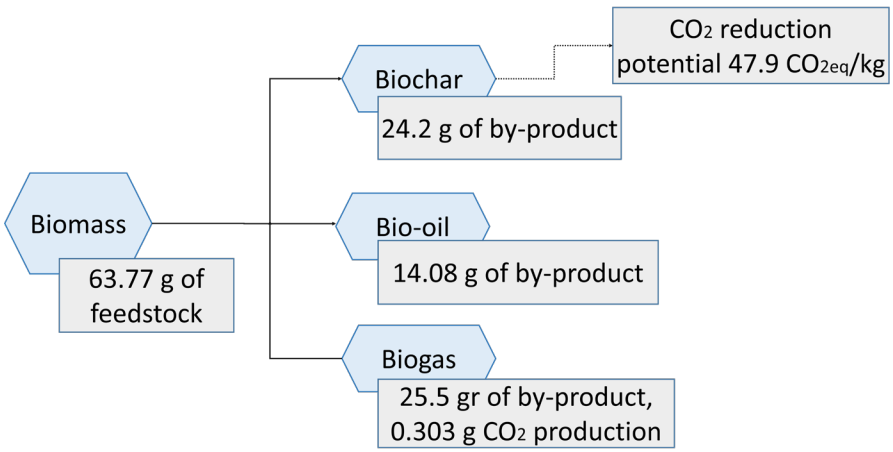

Figure 12: Bioenergy yield balance of SCB using microwave pyrolysis and its $CO_2$ sequestration potential

The life cycle impact assessment of the microwave pyrolysis by-products indicated a carbon dioxide reduction potential of 47.9 $CO_2$eq $kg^{-1}$. Carbon sequestration capacity is related to biochar application, whose purpose is carbon storage.

## 4. Conclusions

This work substantiated that the breakdown of sugarcane bagasse and the energy recovery under microwave pyrolysis are influenced by the input microwave power, susceptor and treatment time. Higher microwave power and susceptor reduce the biochar yield. These operating conditions contribute to increased heating rates and facilitate the formation of volatiles from the bagasse and the thermal breakdown of heavy hydrocarbon, generating more liquid and gas compounds, which can lead to the critical secondary breakdown of oil components into non-condensable volatiles, and hence could conclude that maximum operational conditions were not always the desirable parameters to obtain the optimal bio-oil yield.

## 5. Acknowledgment

The authors are grateful to Wilmar Sugar Australia for supplying the sugarcane bagasse. S.A acknowledges the financial support of the James Cook University Postgraduate Research Scholarship and Cooperative Research Centre for Developing Northern Australia top-up scholarship, which is part of the Australian Government's Cooperative Research Centre Program (CRCP).

## References

Agu, O.S., Tabil, L.G., Mupondwa, E., Emadi, B., Dumonceaux, T. 2022. Impact of Biochar Addition in Microwave Torrefaction of Camelina Straw and Switchgrass for Biofuel Production. *Fuels*, **3**(4), 588-606.

Armando T. Quitain, C.Y.H., Susana Yusup, Mitsuru Sasaki and Yoshimitsu Uemura 2015. Conversion of Biomass to Bio-Oil in Sub- and Supercritical Water. *Biofuels - Status and Perspective*.

Arpia, A.A., Chen, W.-H., Lam, S.S., Rousset, P., de Luna, M.D.G. 2021. Sustainable biofuel and bioenergy production from biomass waste residues using microwave-assisted heating: A comprehensive review. *Chemical Engineering Journal*, **403**, 126233.

Brickler, C.A., Wu, Y., Li, S., Anandhi, A., Chen, G. 2021. Comparing Physicochemical Properties and Sorption Behaviors of Pyrolysis-Derived and Microwave-Mediated Biochar. *Sustainability*, **13**(4), 2359.

Budarin, V.L., Shuttleworth, P.S., De Bruyn, M., Farmer, T.J., Gronnow, M.J., Pfaltzgraff, L., Macquarrie, D.J., Clark, J.H. 2015. The potential of microwave technology for the recovery, synthesis and manufacturing of chemicals from bio-wastes. *Catalysis Today*, **239**, 80-89.

Cai, Z., Ye, F., Xie, Z., Zhang, L., Cui, T. 2021. The choice of cooperation mode in the bioenergy supply chain with random biomass feedstock yield. *Journal of Cleaner Production*, **311**, 127587.

Cheng, F., Luo, H., Colosi, L.M. 2020. Slow pyrolysis as a platform for negative emissions technology: An integration of machine learning models, life cycle assessment, and economic analysis. *Energy Conversion and Management*, **223**, 113258.

Cong, H.B., Masek, O., Zhao, L.X., Yao, Z.L., Meng, H.P., Hu, E.F., Ma, T. 2018. Slow Pyrolysis Performance and Energy Balance of Corn Stover in Continuous Pyrolysis-Based Poly-Generation Systems. *Energy & Fuels*, **32**(3), 3743-3750.

Dai, L., Wang, Y., Liu, Y., He, C., Ruan, R., Yu, Z., Jiang, L., Zeng, Z., Wu, Q. 2020. A review on selective production of value-added chemicals via catalytic pyrolysis of lignocellulosic biomass. *Science of The Total Environment*, **749**, 142386.

Daneshmandi, M., Sahebi, H., Ashayeri, J. 2022. The incorporated environmental policies and regulations into bioenergy supply chain management: A literature review. *Science of The Total Environment*, **820**, 153202.

Duque-Acevedo, M., Belmonte-Ureña, L.J., Cortés-García, F.J., Camacho-Ferre, F. 2020. Agricultural waste: Review of the evolution, approaches and perspectives on alternative uses. *Global Ecology and Conservation*, **22**, e00902.

Ellison, C., McKeown, M.S., Trabelsi, S., Boldor, D. 2017. Dielectric Properties of Biomass/Biochar Mixtures at Microwave Frequencies. *Energies*, **10**(4), 502.

Ethaib, S., Omar, R., Kamal, S.M.M., Biak, D.R.A., Zubaidi, S.L. 2020. Microwave-Assisted Pyrolysis of Biomass Waste: A Mini Review. *Processes*, **8**(9), 1190.

Ferrari, G., Ai, P., Marinello, F., Pezzuolo, A. 2022. Where and how? A comprehensive review of multicriteria approaches for bioenergy plant siting. *Journal of Cleaner Production*, **346**, 131238.

Ferrera-Lorenzo, N., Fuente, E., Bermudez, J.M., Suarez-Ruiz, I., Ruiz, B. 2014. Conventional and microwave pyrolysis of a macroalgae waste from the Agar-Agar industry. Prospects for bio-fuel production. *Bioresour Technol*, **151**, 199-206.

Fodah, A.E.M., Abdelwahab, T.A.M. 2022. Process optimization and technoeconomic environmental assessment of biofuel produced by solar powered microwave pyrolysis. *Scientific Reports*, **12**(1), 12572.

Fodah, A.E.M., Ghosal, M.K., Behera, D. 2021. Studies on Microwave-Assisted Pyrolysis of Rice Straw Using Solar Photovoltaic Power. *BioEnergy Research*, **14**(1), 190-208.

Giorcelli, M., Das, O., Sas, G., Försth, M., Bartoli, M. 2021. A Review of Bio-Oil Production through Microwave-Assisted Pyrolysis. *Processes*, **9**(3), 561.

Gomes, G.M.F.S.D.F.T.N.d.Q.F.Z.J.H.d.Q.F. 2018. Characterization and Potential Evaluation of Residues from the Sugarcane Industry of Rio Grande do Sul in Biorefinery Processes *Natural Resources*, **9**, 175-187.

Halim, S.A., Swithenbank, J. 2016. Characterisation of Malaysian wood pellets and rubberwood using slow pyrolysis and microwave technology. *Journal of Analytical and Applied Pyrolysis*, **122**, 64-75.

Huang, Y.-F., Chiueh, P.-T., Shih, C.-H., Lo, S.-L., Sun, L., Zhong, Y., Qiu, C. 2015. Microwave pyrolysis of rice straw to produce biochar as an adsorbent for CO2 capture. *Energy*, **84**, 75-82.

Huang, Y.F., Chiueh, P.T., Lo, S.L. 2016. A review on microwave pyrolysis of lignocellulosic biomass. *Sustainable Environment Research*, **26**(3), 103-109.

Idris, S.S., Rahman, N.A., Ismail, K., Mohammed Yunus, M.F., Mohd Hakimi, N.I.N. 2022. Microwave-Assisted Pyrolysis of Oil Palm Biomass: Multi-Optimisation of Solid Char

Yield and Its Calorific Value Using Response Surface Methodology. *Frontiers in Chemical Engineering*, **4**.
Inayat, A., Ahmed, A., Tariq, R., Waris, A., Jamil, F., Ahmed, S.F., Ghenai, C., Park, Y.-K. 2022. Techno-Economical Evaluation of Bio-Oil Production via Biomass Fast Pyrolysis Process: A Review. *Frontiers in Energy Research*, **9**.
Juan Camilo Solarte-Toro, Y.C.-P., Carlos Ariel Cardona-Alzate. 2018. Evaluation of biogas and syngas as energy vectors for heat and power generation using lignocellulosic biomass as raw material. *Electronic Journal of Biotechnology*, **33**, 52-62.
Kadlimatti, H.M., Mohan, B.R., M.B.Saidutta. 2019. Bio-oil from microwave assisted pyrolysis of food waste-optimization using response surface methodology. *Biomass and bioenergy*, **123**, 25-33.
Khelfa, A., Rodrigues, F.A., Koubaa, M., Vorobiev, E. 2020. Microwave-Assisted Pyrolysis of Pine Wood Sawdust Mixed with Activated Carbon for Bio-Oil and Bio-Char Production. *Processes*, **8**(11), 1437.
Khuenkaeo, N., Phromphithak, S., Onsree, T., Naqvi, S.R., Tippayawong, N. 2021. Production and characterization of bio-oils from fast pyrolysis of tobacco processing wastes in an ablative reactor under vacuum. *PLoS One*, **16**(7), e0254485.
Kosakowski, W., Bryszewska, M.A., Dziugan, P. 2020. Biochars from Post-Production Biomass and Waste from Wood Management: Analysis of Carbonization Products. *Materials (Basel)*, **13**(21).
Lam, S.S., Wan Mahari, W.A., Ok, Y.S., Peng, W., Chong, C.T., Ma, N.L., Chase, H.A., Liew, Z., Yusup, S., Kwon, E.E., Tsang, D.C.W. 2019. Microwave vacuum pyrolysis of waste plastic and used cooking oil for simultaneous waste reduction and sustainable energy conversion: Recovery of cleaner liquid fuel and techno-economic analysis. *Renewable and Sustainable Energy Reviews*, **115**, 109359.
Le Pera, A., Sellaro, M., Bencivenni, E. 2022. Composting food waste or digestate? Characteristics, statistical and life cycle assessment study based on an Italian composting plant. *Journal of Cleaner Production*, **350**, 131552.
Lee, S.Y., Sankaran, R., Chew, K.W., Tan, C.H., Krishnamoorthy, R., Chu, D.-T., Show, P.-L. 2019. Waste to bioenergy: a review on the recent conversion technologies. *BMC Energy*, **1**(1), 4.
Leng, L., Xiong, Q., Yang, L., Li, H., Zhou, Y., Zhang, W., Jiang, S., Li, H., Huang, H. 2021. An overview on engineering the surface area and porosity of biochar. *Sci Total Environ*, **763**(144204), 144204.
Li, H.Y., Huang, Y.F., Lin, X.H., Liu, Y.F., Lv, Y., Liu, M.H., Zhang, Y.M. 2022a. Microwave-assisted depolymerization of lignin with synergic alkali catalysts and a transition metal catalyst in the aqueous system. *Reaction Chemistry & Engineering*, **7**(8), 1750-1761.
Li, J., Dai, J.J., Liu, G.Q., Zhang, H.D., Gao, Z.P., Fu, J., He, Y.F., Huang, Y. 2016. Biochar from microwave pyrolysis of biomass: A review. *Biomass & Bioenergy*, **94**, 228-244.
Li, J., Li, L., Suvarna, M., Pan, L., Tabatabaei, M., Ok, Y.S., Wang, X. 2022b. Wet wastes to bioenergy and biochar: A critical review with future perspectives. *Science of The Total Environment*, **817**, 152921.
Li, X., Li, K., El-Mashad, H., Jenkins, B.M., Yin, W. 2018. White poplar microwave pyrolysis: Heating rate and optimization of biochar yield. *BioResources*, **13**(1), 1107-1121.
Lin, B., W.Chen. 2015. Sugarcane bagasse pyrolysis in a carbon dioxide atmosphere with conventional and microwave-assisted heating. *Front. Energy Res*, **4**.
Liu, T., Miao, P., Shi, Y., Tang, K.H.D., Yap, P.-S. 2022. Recent advances, current issues and future prospects of bioenergy production: A review. *Science of The Total Environment*, **810**, 152181.
Liu, Y., Chen, S., Chen, A.Y., Lou, Z. 2021. Variations of GHG emission patterns from waste disposal processes in megacity Shanghai from 2005 to 2015. *Journal of Cleaner Production*, **295**, 126338.
Liyana, Z., Malek, F., Nornikman, H., Affendi, N.A.M., Mohamed, L., Saudin, N., Ali, A.A. 2012. Investigation of sugar cane bagasse as alternative material for pyramidal microwave

absorber design. *2012 IEEE Symposium on Wireless Technology and Applications (ISWTA)*, Bandung.
Lo, S.L., Huang, Y.F., Chiueh, P.T., Kuan, W.H. 2017. Microwave pyrolysis of lignocellulosic biomass. *8th International Conference on Applied Energy (Icae2016)*, **105**, 41-46.
Lyu, G., Wu, S., Zhang, H. 2015. Estimation and Comparison of Bio-Oil Components from Different Pyrolysis Conditions. *Frontiers in Energy Research*, **3**(28).
M.Waqasa, A.S.Aburiazaiza, R.Minadad, M.Rehan, M.A.Barakat, A.S.Nizami. 2018. Development of biochar as fuel and catalyst in energy recovery technologies. *Journal of Cleaner Production*, **188**, 477-488.
Mierzwa-Hersztek, M., Gondek, K., Jewiarz, M., Dziedzic, K. 2019. Assessment of energy parameters of biomass and biochars, leachability of heavy metals and phytotoxicity of their ashes. *Journal of Material Cycles and Waste Management*, **21**, 786–800.
Mohammed, I.Y., Abakr, Y.A., Kazi, F.K., Yusuf, S., Alshareef, I., Chin, S.A. 2015. Pyrolysis of Napier Grass in a Fixed Bed Reactor: Effect of Operating Conditions on Product Yields and Characteristics. *Bioresources*, **10**(4), 6457-6478.
Mong, G.R., Chong, C.T., Ng, J.-H., Chong, W.W.F., Ong, H.C., Tran, M.-V. 2021. Multivariate optimisation study and life cycle assessment of microwave-induced pyrolysis of horse manure for waste valorisation and management. *Energy*, **216**, 119194.
Mong, G.R., Liew, C.S., Chong, W.W.F., Mohd Nor, S.A., Ng, J.-H., Idris, R., Chiong, M.C., Lim, J.W., Zakaria, Z.A., Woon, K.S. 2022. Environment impact and bioenergy analysis on the microwave pyrolysis of WAS from food industry: Comparison of CO2 and N2 atmosphere. *Journal of Environmental Management*, **319**, 115665.
Mullane, J. 2022. Average Electricity Costs per kWh, Canstar Blu.
Najeeb, M.I., Sultan, M.T.H., Andou, Y., Shah, A.U.M., Eksiler, K., Jawaid, M., Ariffin, A.H. 2021. Characterization of Lignocellulosic Biomass from Malaysian's Yankee Pineapple AC6 Toward Composite Application. *Journal of Natural Fibers*, **18**(12), 2006-2018.
Nizamuddin, S., Baloch, H.A., Siddiqui, M.T.H., Mubarak, N.M., Tunio, M.M., Bhutto, A.W., Jatoi, A.S., Griffin, G.J., Srinivasan, M.P. 2018. An overview of microwave hydrothermal carbonization and microwave pyrolysis of biomass. *Reviews in Environmental Science and Bio/Technology*, **17**, 813–837.
Panwar, N.L., Paul, A.S. 2021. An overview of recent development in bio-oil upgrading and separation techniques. *Environmental Engineering Research*, **26**(5), 200382-0.
Pham, T.N., Sooknoi, T., Crossley, S.P., Resasco, D.E. 2013. Ketonization of Carboxylic Acids: Mechanisms, Catalysts, and Implications for Biomass Conversion. *Acs Catalysis*, **3**(11), 2456-2473.
Prasad, S., Ingle, A.P. 2019. Chapter 12 - Impacts of sustainable biofuels production from biomass. in: *Sustainable Bioenergy*, (Eds.) M. Rai, A.P. Ingle, Elsevier, pp. 327-346.
Quillope, J.C.C., Carpio, R.B., Gatdula, K.M., Detras, M.C.M., Doliente, S.S. 2021. Optimization of process parameters of self-purging microwave pyrolysis of corn cob for biochar production. *Heliyon*, **7**(11), e08417.
Rover, M.R. 2013. Analysis of sugars and phenolic compounds in bio-oil, Vol. Doctor of philosophy, Iowa State University, pp. 134.
S, M.S., Paramasivan, B. 2021. Evaluation of influential factors in microwave assisted pyrolysis of sugarcane bagasse for biochar production. *Environmental Technology & Innovation*, **24**, 101939.
S.Mutsengerere, C.H.Chihobo, D.Musademba, I.Nhapi. 2019. A review of operating parameters affecting bio-oil yield in microwave pyrolysis of lignocellulosic biomass. *Renewable and Sustainable Energy Review*, **104**, 328-336.
Sainab Omar, S.A., Yang Yang, Jiawei Wang. 2019. Production of renewable fuels by blending bio-oil with alcohols and upgrading under supercritical conditions. *Front. Chem. Sci. Eng.* , **13**(4), 702–717.
Sakhiya, A.K., Anand, A., Kaushal, P. 2020. Production, activation, and applications of biochar in recent times. *Biochar*, **2**, 253-285.
Selvam S, M., Paramasivan, B. 2022. Microwave assisted carbonization and activation of biochar for energy-environment nexus: A review. *Chemosphere*, **286**, 131631.

Shi, K., Yan, J., Menéndez, J.A., Luo, X., Yang, G., Chen, Y., Lester, E., Wu, T. 2020. Production of H2-Rich Syngas From Lignocellulosic Biomass Using Microwave-Assisted Pyrolysis Coupled With Activated Carbon Enabled Reforming. *Frontiers in Chemistry*, **8**.

Shin Ying Foong, N.S.A.L., Rock Keey Liew, Peter Nai Yuh Yek, Su Shiung Lam. 2020. Production of biochar for potential catalytic and energy applications via microwave vacuum pyrolysis conversion of cassava stem. *Materials Science for Energy Technologies*, **3**, 728-733.

Shukla, N., Sahoo, D., Remya, N. 2019. Biochar from microwave pyrolysis of rice husk for tertiary wastewater treatment and soil nourishment. *Journal of Cleaner Production*, **235**, 1073-1079.

Si, Z., Zhang, X., Wang, C., Ma, L., Dong, R. 2017. An Overview on Catalytic Hydrodeoxygenation of Pyrolysis Oil and Its Model Compounds. *Catalysts*, **7**(6), 169.

Sieng-Huat Kong; Su Shiung Lam; Peter Nai Yuh Yek; Rock Keey Liew; Nyuk Ling Ma; Mohammad Shahril Osman; Chee Chung Wong. 2018. Self-purging microwave pyrolysis: an innovative approach to convert oil palm shell into carbon-rich biochar for methylene blue adsorption. *Chemical Technology and Biotechnology*, **94**(5), 1397-1405.

Supramono, D., Fachriza, N., Devina, Y.M. 2015. Microwave Pyrolysis of Sugarcane Bagasse for Bio-Oil Production. *Conference: Seminar Nasional Teknik Kimia Indonesia 2015. Sustainable Energy and Mineral Processing for National Competitiveness*, Yogyakarta.

Suriapparao, D.V., Batchu, S., Jayasurya, S., Vinu, R. 2018. Selective production of phenolics from waste printed circuit boards via microwave assisted pyrolysis. *Journal of Cleaner Production*, **197**, 525-533.

Suriapparao, D.V., Kumar, D.A., Vinu, R. 2022. Microwave co-pyrolysis of PET bottle waste and rice husk: effect of plastic waste loading on product formation. *Sustainable Energy Technologies and Assessments*, **49**, 101781.

Suriapparao, D.V., Pradeep, N., Vinu, R. 2015. Bio-Oil Production from Prosopis juliflora via Microwave Pyrolysis. *Energy & Fuels*, **29**(4), 2571-2581.

Suzanne Anouti, G.H., Maxime Deniel, Anne Roubaud. 2016. Analysis of Physicochemical Properties of Bio-Oil from Hydrothermal Liquefaction of Blackcurrant Pomace. *Energy and Fuels, American Chemical Society*, **30**(1), 398-406.

Tomczyk, A., Sokolowska, Z., Boguta, P. 2020. Biochar physicochemical properties: pyrolysis temperature and feedstock kind effects. *Reviews in Environmental Science and Bio-Technology*, **19**(1), 191-215.

Ubiera, L., Polaert, I., Delmotte, M., Abdelouahed, L., Taouk, B. 2021. Energy optimization of bio-oil production from biomass by fast pyrolysis using microwaves. *Reaction Chemistry & Engineering*, **6**(10), 1884-1899.

Venkatesh, G., Gopinath, K.A., Reddy, K.S., Reddy, B.S., Prabhakar, M., Srinivasarao, C., Visha Kumari, V., Singh, V.K. 2022. Characterization of Biochar Derived from Crop Residues for Soil Amendment, Carbon Sequestration and Energy Use. *Sustainability*, **14**(4), 2295.

Wallace, C.A., Afzal, M.T., Saha, G.C. 2019. Effect of feedstock and microwave pyrolysis temperature on physio-chemical and nano-scale mechanical properties of biochar. *Bioresources and Bioprocessing*, **6**(33).

Wang, L., Lei, H., Ruan, R. 2015. Techno-Economic Analysis of Microwave-Assisted Pyrolysis for Production of Biofuels. in: *Production of Biofuels and Chemicals with Microwave*, (Eds.) Z. Fang, J.R.L. Smith, X. Qi, Springer Netherlands. Dordrecht, pp. 251-263.

Wang, S., Guo, Z., Cai, Q., Guo, L. 2012. Catalytic conversion of carboxylic acids in bio-oil for liquid hydrocarbons production. *Biomass and Bioenergy*, **45**, 138-143.

Wang, X.Y., Wu, F.Y., Li, C., Chen, M.Q., Wang, J. 2018. High Quality Bio-oil Production from Catalytic Microwave-assisted Pyrolysis of Pine Sawdust. *Bioresources*, **13**(3), 5479-5490.

Wang, Z., Burra, K.G., Lei, T., Gupta, A.K. 2021. Co-pyrolysis of waste plastic and solid biomass for synergistic production of biofuels and chemicals-A review. *Progress in Energy and Combustion Science*, **84**, 100899.

Wattanasilp, C., Songprakorp, R., Nopharatana, A., Khompatraporn, C. 2021. Techno-Cost-Benefit Analysis of Biogas Production from Industrial Cassava Starch Wastewater in Thailand for Optimal Utilization with Energy Storage. *Energies*, **14**(2), 416.

Y. Zhang, P.C., Liu, S., L. Fan, N.Z., Min, M., Cheng, Y., Peng, P., Anderson, E., Wang, Y., Wan, Y., Liu, Y., Li, B., Ruan, R. 2017. Microwave-Assisted Pyrolysis of Biomass for Bio-Oil Production. in: *Pyrolysis*, Mohamed Samer, IntechOpen, pp. 129-166.

Yaning Zhang, P.C., Shiyu Liu, Liangliang Fan, Nan Zhou, Min Min, Yanling Cheng, Peng Peng, Erik Anderson, Yunpu Wang, Yiqin Wan, Yuhuan Liu, Bingxi Li and Roger Ruan. 2017. Microwave-Assisted Pyrolysis of Biomass for Bio-Oil Production. in: *Pyrolysis*, (Ed.) M. Samer. ntechOpen.

Yu, H., Qu, J., Liu, Y., Yun, H., Li, X., Zhou, C., Jin, Y., Zhang, C., Dai, J., Bi, X. 2022. Co-pyrolysis of biomass and polyvinyl chloride under microwave irradiation: Distribution of chlorine. *Science of The Total Environment*, **806**, 150903.

Yu, Y., Chua, Y.W., Wu, H.W. 2016. Characterization of Pyrolytic Sugars in Bio-Oil Produced from Biomass Fast Pyrolysis. *Energy & Fuels*, **30**(5), 4145-4149.

Zhang, S., Xiong, Y. 2016. Washing pretreatment with light bio-oil and its effect on pyrolysis products of bio-oil and biochar. *RSC Adv.*, **6**(7), 5270-5277.

Zhang, X., Xiang, W., Miao, X., Li, F., Qi, G., Cao, C., Ma, X., Chen, S., Zimmerman, A.R., Gao, B. 2022. Microwave biochars produced with activated carbon catalyst: Characterization and sorption of volatile organic compounds (VOCs). *Science of The Total Environment*, **827**, 153996.

Zhang, X.S., Rajagopalan, K., Lei, H.W., Ruan, R., Sharma, B.K. 2017a. An overview of a novel concept in biomass pyrolysis: microwave irradiation. *Sustainable Energy & Fuels*, **1**(8), 1664-1699.

Zhang, Y., Chen, P., Liu, S., Fan, L., Zhou, N., Min, M., Cheng, Y., Peng, P., Anderson, E., Wang, Y., Wan, Y., Liu, Y., Li, B., Ruan, R. 2017b. Microwave-Assisted Pyrolysis of Biomass for Bio-Oil Production. in: *Pyrolysis*, (Ed.) M. Samer, IntechOpen, pp. 129-166.

Zhao, Z., Jiang, Z., Xu, H., Yan, K. 2021. Selective Production of Phenol-Rich Bio-Oil From Corn Straw Waste by Direct Microwave Pyrolysis Without Extra Catalyst. *Frontiers in Chemistry*, **9**(489).

Zi, W., Chen, Y., Pan, Y., Zhang, Y., He, Y., Wang, Q. 2019. Pyrolysis, morphology and microwave absorption properties of tobacco stem materials. *Sci Total Environ*, **683**, 341-350.